A scalable approach to indoor localization using existing ZigBee reference devices

Derks, H.B.M.

Award date:
2011

AME

TU/e Technische Universiteit Eindhoven University of Technology

Master's thesis

A scalable approach to indoor localization using existing ZigBee reference devices

Author: ing. H.B.M. Derks

Date: August 18, 2011

Assessment committee: prof.dr.ir. T. Basten, prof.dr. J.J. Lukkien, ir. M.G.J.R. Stalpers

company confidential

Abstract

If someone wants to localize a person or object in a building, then in the worst case all rooms must be visited in order to find the person or object. An electronic means to support indoor localization would be useful. The existing Global Positioning System (GPS) does not cover indoor areas for localization. This is a pity since it is known from the U.S. Environmental Protection Agency, that people spend almost 90 percent of their time indoors.

A solution to the indoor localization problem is proposed in this thesis. The goal is to develop a real time localization system which is applicable for tracking persons or objects in an indoor site. Other applications can be navigating in a mall or hospital.

It is assumed that the localization area is equipped with AME ZigBee devices. ZigBee is a low data rate, low-power and secure radio protocol. For example, AME designed ZigBee devices used for wireless socket switches. In the context of indoor localization, AME ZigBee socket switches are called *reference nodes*. Also, it is assumed that the person carries a tag. The tag, denoted as *blind node*, is a battery powered AME ZigBee device. The blind node the node that is supposed to localize itself.

The localization technique used by GPS is multilateration. Based on distances to reference positions, goniometry is used to calculate a location. Unfortunately, distances between two ZigBee radios cannot be determined accurately enough. The transmit time of a ZigBee message could be used for distance determination, since a signal propagates with the speed of light. However, transmit time (magnitude of nanoseconds) cannot be measured accurately enough. Also the power of a signal correlates to distance, but is also not applicable because of reflections causing multipath propagation. This means that signal paths do not all end up at the receiver: thus multilateration is not applicable for localization using ZigBee.

Fact is that as long as the environment stays static, the reflections are also static. The localization scheme proposed in this thesis is based on static reflections. The expected received power of each position in a localization area is extracted by a *training phase* which is done *a priori*. The training phase is done using multiple blind nodes, and results in a model containing values for the expected received power per reference node, for each position in the localization area. In the *localization phase*, the measured received power values from messages of reference nodes are used to compare to the model, to determine a location. The proposed localization system performs with a median error of at most $3m$. Using multiple radios at the blind node improves the median error to at most $2m$. An implementation of a single radio blind node has been made.

The Achilles heel of the system is that major changes in a localization area can disturb localization significantly, i.e. only small movements of obstacles are allowed.

Acknowledgements

Finishing the master project has been made possible by many people.

I thank the company Applied Micro Electronics "AME" BV for giving me the opportunity to do the master project. AME is a company in the field of electronics and IT. The master project took place at the Embedded Systems group of software department called AME-SolvIT. I thank my colleagues of the Embedded Systems group for supporting me solving programming problems. In special, I thank Micha Stalpers and Bram van Nunen for interesting discussions, guidance, valuable input and unconditional support.

Secondly, I thank S.V. Heythuysen for allowing me to perform experiments on one of their football fields.

Last but not least, I thank supervisor Twan Basten from the Eindhoven University of Technology for giving input, guidance and making this thesis more readable.

Contents

List Of Acronyms

ABP Area-Based Probability

CDF Cumulative Distribution Function

CSS Chirp Spread Spectrum

ESD Electrostatic Discharge

IC Integrated Circuit

FP Fingerprint

FM Frequency Modulation

GPS Global Positioning System

GSM Global System for Mobile communication

LoS Line of Sight

PCB Printed Circuit Board

RF Radio Frequency

RSS Received Signal Strength

RSSI Received Signal Strength Indication

RTLS Real Time Locating System

SDS-TWR Symmetric Double Sided Two Way Ranging

TDoA Time Difference of Arrival

ToF Time of Flight

UWB Ultra-Wideband

Wi-Fi Wireless Fidelity

WSN Wireless Sensor Network

1 Introduction

During the last decade, location based services have become more and more important. Location based services include navigation, location based marketing, and asset tracking. For outdoor environments, there is the Global Positioning System (GPS). However, environments like parking lots, logistic terminals, shopping malls and other indoor environments are not covered by GPS. Inspired by the lack of an indoor Realtime Location System (RTLS), this thesis is written.

The thesis proposes an indoor localization system based on ZigBee, a wireless sensor network (WSN) technology. A WSN consists of spatially distributed electronic devices which can communicate over short distances. A device in a WSN, denoted *node*, is equipped with a radio transceiver to communicate with other nodes. Based on presence of neighboring nodes, a mobile node can localize itself. The proposed localization system localizes people and objects in an indoor site, with median accuracy of 2-3m in 2D space.

In the remainder of this thesis, a mobile device which is supposed to locate itself is named a *blind node*. A blind node "listens" to the network in order to determine its location. The other nodes in a network are assumed to have a static location and are called *reference nodes*.

The remainder of this section describes the problem statement and lists the requirements for the localization system to be designed. Related work in the field of localization is outlined, and the research direction for the thesis is motivated. The contributions of the thesis are summarized and the outline of the remainder of this document is given.

1.1 Requirements

An RTLS is a system that provides realtime identification of the location of objects or persons. The problem is that there is not yet a robust, accurate system which can localize persons in the range of ZigBee wireless sensor networks in an indoor environment. The need for an indoor RTLS is reinforced by the fact that people spend 80 % - 90 % of their time indoors [12].

The location system developed during the thesis meets the following requirements.

1. The system must be suitable for realtime person location tracking. This requires an accuracy of approximately 3m in office environments.
2. Adoptability of the system of existing AME ZigBee devices, to maximize the scope of application. Obviously, the AME ZigBee network should retain its operation. Hardware changes to existing reference nodes is not allowed, but software updates ware allowed.

3. The system must support tracking of multiple persons or objects.
4. The blind node's environmental knowledge is minimized. Only the location of reference nodes, or a training phase extracting site metrics is allowed to be assumed. The installation of the system may take at most one day for sites comparable to the AME building ($5000m^2$ of office space). Again, the reason is to maximize the application scope.
5. Enhancements for specific locations, e.g. no-go areas or hot-spot tracking are desired.
6. This requirement is derived from Requirement 3 (Scalability in nr. of blind nodes), since the network load is limited. The calculation of the location of a blind node must be done by the blind node itself. That means that there is no offline processing. This is to allow scalability in number of blind nodes and to minimize costs.

As Requirement 1 (Suitable for realtime person tracking)states, the system should enable localization for person tracking in an office environment. AME's building is used for testing, which is a two floor building. Thus, the system should be able to distinguish areas, where a floor or hall can be interpreted as an area.

The intended hardware for a blind node is an AME Sensor Node. A AME Sensor Node is an AME ZigBee operated device intended to be carried by people or objects. The dimensions are dimensions are 78x48x20mm. The embedded software of the AME Sensor Node can be updated over-the-air. An additional PCB can be mounted to the AME Sensor Node. For example, the additional PCB can contain an additional ZigBee radio to improve localization accuracy.

1.2 Related work and chosen research direction

Since realtime indoor localization is a new and hot topic in current research, there are no books available describing indoor localization techniques. There are more and more conferences concerning localization, like the International Conference on Positioning and Context-Awareness (PoCA) held on March 24th 2011 in Brussels, Belgium and the International Conference on Indoor Positioning and Indoor Navigation (IPIN) to be held on 21-23 September 2011 in Guimarães, Portugal.

At the moment of writing, articles are being released concerning context awareness and localization. In scientific research, a lot of effort has been invested in localization using Wi-Fi, WSN, FM, (Ultra Wide Bandwidth) UWB, ultrasound and even using temperature. Using UWB, the company Ubisense (`http://www.ubisense.net`) offers a commercial RTLS for automotive and aerospace manufacturing. The system has "sub-meter" accuracy in 3D.

However, there is not yet a localization technique for WSN's that is widely accepted, nor in industry, nor in science. For WSN's there is a localization technique called fingerprinting, which is the basis for this thesis. Chapter 2 describes the state of the art localization

techniques. Often research of localization in WSN's focusses on high accuracy systems requiring expensive dedicated hardware. In a lot of cases, this leads to superfluous accuracy in an unrealistic lab environment. For example, in [9] and [10], the authors assume a line of sight between blind nodes and reference nodes. This cannot be assumed in practice since objects and humans interrupt the line of sight. Also, *Schwarzer et al.* [13] use dedicated hardware which enables 2D localization with $0.16m$ accuracy. This dedicated hardware is not desirable because of costs and non-adoptability by existing WSN nodes.

The goal of this thesis is to present:

A *scalable* indoor location tracking system with room-level accuracy ($3m$)

The context of scalable is the number of blind nodes. This means that the network traffic should stay constant, when adding a blind node to the network.

1.3 Contributions

In addition to the field's knowledge this thesis has proposed a scalable, practically applicable localization system. In short, the proposed system offers a scalable solution to indoor localization which can be adopted in existing AME ZigBee networks. Besides over-the-air fingerprint database and algorithm updates, a blind node's localization median accuracy can be increased to $2m$ using additional antennas. A detailed description of the contributions of this thesis can be found in Section 6.1.

1.4 Outline

The remainder of this thesis is as follows. Chapter 2 describes related work in the field of indoor localization in WSN. It turns out that signal strength is applicable to existing AME ZigBee products. Detailed experiments are described in Chapter 3. Based on the findings concerning signal strength, Chapter 4 describes the localization scheme presented by this thesis. The proposed localization scheme is evaluated in Chapter 5. Finally Chapter 6 provides some discussion and concludes this thesis.

2 Localization techniques in WSN

Since the early 90s, research in indoor localization has been done. This section describes an overview of existing localization techniques. Localization techniques can be divided into two classes called *range* and *range free* methods [4]. Range methods use distances between mobile node and reference positions to calculate the location by goniometry. The class of range free methods is not based on distances; they use for example area probability in order to calculate a location.

According to [15], a blind node in a localization system can be an *active* or *passive* mobile device.

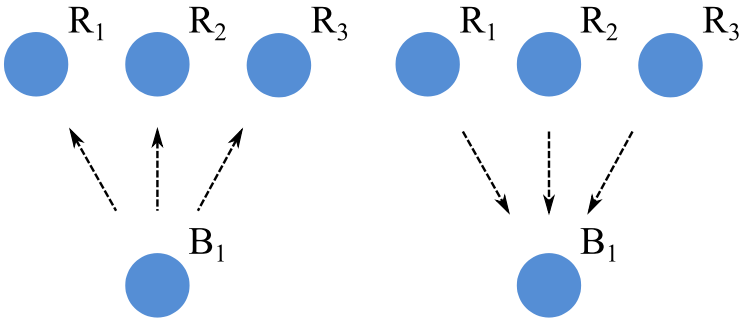

(a) Active blind node (b) Passive blind node

Figure 1: Active- and passive mobile node.

In Figure 1a, an active blind node is shown, where the blind node periodically broadcasts a message. The reference nodes receive these messages and send them to a central server which calculates the location. Depending on the application, the calculated location is sent back to the blind node. Figure 1b shows a passive blind node, which receives messages from reference nodes. The reference nodes send periodically their identity or position. In this case, a blind device determines its location by itself. In contrast to the active configuration, a blind node operating as an passive blind node will lead to less network overhead. An passive operating blind node is preferred, in order to fulfill Requirement 3 (Scalability in nr. of blind nodes). Note that there are variants where there is two-way communalization [19].

Because of Requirement 6 (Calculations by blind node) given in Section 1.1, the localization methods described in this section are described from the perspective that the blind node operates as a passive mobile device.

This section describes the main range methods, which can be divided in Time of Flight (ToF) based methods and signal power based method. The range free methods considered are Angle of Arrival and a signal power fingerprinting method. This sections ends with a survey and assessment of these existing localization techniques.

2.1 Range methods

The basis for range methods is the knowledge of absolute distances to reference locations. When a distance of d meters from the blind node to a reference location is known, one can draw a circle around the reference location, indicating all locations which are located d meters from the reference location. The intersecting point of the circles is the location where the blind node is located.

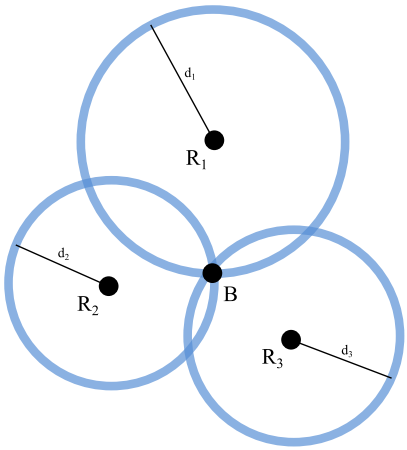

Figure 2: Trilateration uses distances to reference nodes.

Figure 2 illustrates a situation where the distances d_1, d_2 and d_3 to reference locations respectively R_1, R_2 and R_3 are known. Trilateration determines the blind node's location to be the intersecting point of the circles. Since two circles can have two intersection, at least one additional circle is needed. Therefore a minimum of three distances to references nodes is required to determine the location of the blind nod. Because of inaccuracy of single distance estimations, multilateration is a generalized version of trilateration supporting multiple reference positions, to achieve more localization accuracy [14].

The range methods described in this section determine distances from the blind node to reference nodes. Note that the following conditions must hold in order to use multilateration.

- Location of reference nodes must be known.
- Location of reference nodes must be static.

For range methods, Time of Flight based methods and the signal power method are described in the following subsections.

2.1.1 Time of Flight based methods

A relatively accurate localization system is the Global Positioning System (GPS), for example used in car navigation. There are 31 GPS satellites placed around the globe at a height of 20.000 km, transmitting RF signals. The physical distance to satellites can be determined based on time measurements and the transmission speed (speed of light, c_0). If the distance to three or more satellites is known, multilateration can be used to determine the location. Similar time based techniques can be used in WSN's.

Roundtrip Time of Flight (RTOF) is a derivative of ToF, since it does two time measurements. RToF measures the Roundtrip Time τ_B and the processing time τ_R as illustrated by Figure 3.

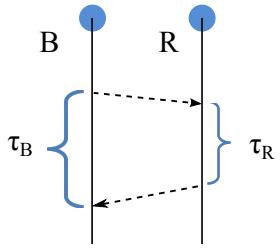

Figure 3: Roundtrip Time of Flight.

The difference $\tau_B - \tau_R$ equals twice the propagation time. The distance between blind and reference node can be calculated using Equation 1.

$$d = \frac{\tau_B - \tau_R}{2} \cdot c_0 \tag{1}$$

In the RTOF technique, there is two-way communication between the blind node and the reference nodes. This means that the blind node is not clearly in an active of passive mobile device.

Previous work in [19] shows distance RToF based estimation with an error of $1.6m$. ToF methods are certainly applicable methods for distance estimation between nodes in a WSN. However, they require high precision time measurement. The speed of signal propagation is equal to c_0, resulting in small transmit times. Commonly available ZigBee architectures do not support the required time accuracy.

Similar to ToF in WSN, localization systems based on the ultrasound technology typically use ToF. Unfortunately ultrasound radios are not standard supported by ZigBee compliant Intergraded Circuits (IC's), thus Requirement 2 (Adoptability of existing AME ZigBee devices) prohibits use of ultrasound.

Although there is no widely accepted localization technique for WSN, the company Nanotron [16] offers a distance measurement which can be generalized to 2D or 3D localization. The technique of Nanotron comes back to RToF, but differs in frequency modulation. It is a variant using double RToF, also known as Symmetric Double Sided Two Way Ranging (SDS-TWR). Both blind and reference node are measuring time spans and compute their mutual distance using Equation 1. The calculated distances are averaged in order to estimate the distance. This leads to an accuracy of distance estimation within $1m$, even in the most challenging environments.

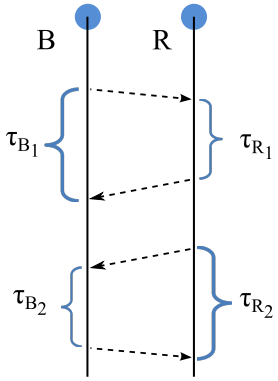

Figure 4: Symmetric Double Sided Two Way Ranging uses double RToF.

Figure 4 shows a scheme of SDS-TWR. As with RToF, a blind node has two-way communication with reference nodes. This limits scalability due to network traffic growth, when adding a blind node to the network.

SDS-TWR provides protection against noise by the Chirp Spread Spectrum (CSS) modulation technique. CSS is a spread spectrum technique that uses a wideband frequency. The wider the signals bandwidth, he narrower the correlation peaks. Making the correlation peak as narrow as possible increases the time resolution of the method [16]. Also, Nanotron's technique is not applicable for this thesis since the available Nanotron IC (nanoLOC TRX Transceiver) on the market does not support ZigBee. Since the nanoLOC TRX Transceiver operates in the same frequency band as ZigBee ($2.4GHz$), one could implement the ZigBee stack. However, implementing the ZigBee stack is very time consuming. Besides the lack of support for ZigBee, the Nanotron system requires additional hardware for reference nodes which was prohibited by Requirement 2 (Adoptability of existing AME ZigBee devices).

2.1.2 Signal power

An RF signal sent at a certain carrier frequency is always sent with a certain amount of power. Propagating through air, the signal's power decreases. As a consequence, signal

power correlates to the distance between sender and receiver. This implies that distances can be determined based on received signal power.

The theoretical correlation between received signal power, denoted Received Signal Strength (RSS) in dBm, and distance d is described by [1] in Equation 2.

$$RSS(d) = -(10n \cdot \log_{10} d + A) \tag{2}$$

In the formula, n denotes the signal propagation, which is influenced by thickness of walls and other environmental conditions. For ease of modeling, n is often treated as constant. For a given deployment, the variable n can be determined experimentally. Errors in n can cause inaccurate distance calculation. Parameter A denotes the received signal strength at one meter distance. This parameter can also experientially be determined. Parameter d denotes the distance between sender and receiver in meters. Based on distance calculation using Equation 2 and multilateration, localization can be done.

Assuming this theory holds in practice, *Lau and Chung* positioned their blind node in line of sight (LoS) to reference nodes [9]. In both indoor and outdoor environments, experiments they have done resulted in a 2D localization error of $3m$.

The localization error of $3m$ is acceptable, but the assumption that reference nodes are placed in line of sight is not. If there is no LoS to reference nodes, the drawback arises that a signal's power is affected by reflections and interferences, which causes inaccurate distance estimations.

2.2 Range free methods

Range free localization methods compute a location, not using distance estimation. This means that not all range free methods do require knowledge of the location on the reference nodes. The following sections describe the Angle of Arrival and an RSS fingerprinting method. Angle of Arrival is a novel technique using rotating antennas [10]. Signal power fingerprinting compares RSS measurements to a model. Other range free methods are not known at the moment of writing.

Both range free methods assume that the location of the reference nodes is static. Moreover, the Angle of Arrival method assumes that the location of the reference nodes must be known.

2.2.1 Angle of Arrival

The Angle of Arrival (AoA) method determines angles in order to calculate the location of the blind node. Using directional synchronously rotating antennas at reference nodes, a blind node can determine angles of arrivals. This can be explained by means of Figure 5.

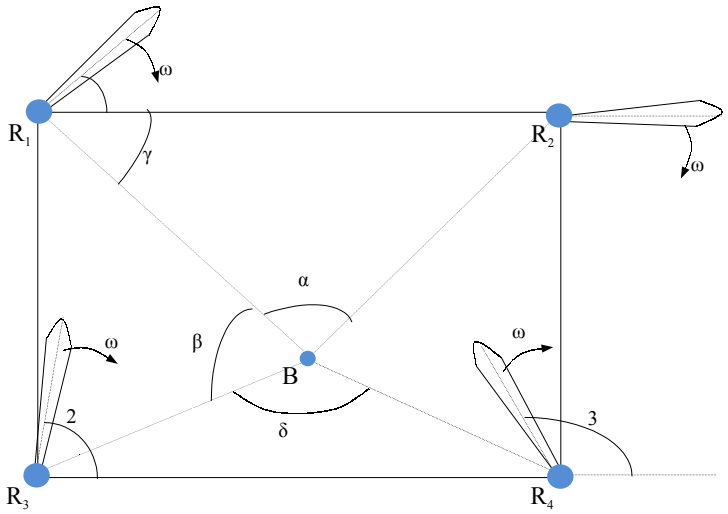

Figure 5: Angle of arrival (AoA).

The reference nodes are equipped with directional antennas, which are rotating at equal speed. The time difference of arrival of beams from reference nodes is proportional to the angle the blind node makes in for example $\triangle BR_1R_2$. Goniometry can be used for location estimation. Note that locations of reference need to be known. The work of [10] resulted in a localization error of roughly 2m, in 2D space. The work is limited to simulation only.

Although the idea of directional rotating antennas is innovative, the practical objections are unacceptable. These objections include the need for mechanical rotating antennas and communication of blind node and reference node with the line of sight assumption. Also, clock synchronization is needed which implies additional network traffic [7].

2.2.2 Fingerprinting signal power

It is generally known that signal power relates to distances. However, it is not generally known that signal power can also be used for fingerprinting.

In the fingerprinting technique, for each location (x, y) in the localization area there is a set of expected signal power values for all reference nodes. A set of expected signal power values for a given location, is called a *fingerprint*.

The set of fingerprints of all locations in the localization area is called the *fingerprint database*. The fingerprint database is built *a priori* by a training phase, or calculation [3]. A blind node can localize itself using the "live" signal power values measured from messages from neighboring reference nodes. These live signal power values are compared to the fingerprint database, in order to find the best matching fingerprint from the database. Then, the best matching fingerprint corresponds to the location of the blind node.

Part of the work of *Weyn* [17] implements fingerprinting. The author combines GPS, Wi-Fi, and GSM for localization for both indoor and outdoor application. For indoor environments the Wi-Fi technology is used for fingerprinting. A blind node in the proposed solution can localize itself within $3m$ in 2D.

2.3 Survey

The most important requirement for this thesis is adoptability of the system, i.e. how easy can it be used in existing AME ZigBee networks? The comparative study is summarized by Table 1. Assuming all localization techniques described are suitable for person tracking (Requirement 1 (Suitable for realtime person tracking)), the following table is made.

Table 1: Comparison of localization techniques

	Range methods		Range free methods	
Name / property	ToF based methods	Signal power	AoA	Fingerprinting signal power
no need for additional hardware hardware for reference nodes	✗	✓	✗	✓
no need for clock synchronization	✓	✓	✗	✓
accuracy (dimension)	3m (2D)	3m (2D)	?	3m (2D)
ignore location of reference nodes	✗	✗	✗	✓
additional network load	⋆⋆	⋆	⋆	⋆
notes		LoS	simulation	*a priori* work

The localization techniques are assessed based on the requirements. Requirement 2 (Adoptability of existing AME ZigBee devices) prohibits the use of additional hardware of reference nodes, and this requirement also includes the ease of installation. For ease of installation, it is preferred that the locations of reference nodes are not required to be known, and *a priori* work is not desired. Requirement 6 (Calculations by blind node) is derived from Requirement 2 (Adoptability of existing AME ZigBee devices) and tries to minimize the additional network overload. The need for clock synchronization is directly related to network overload and additional hardware, since clock synchronization comes with a price in terms of network overload and additional hardware [18]. Requirement 3 (Scalability in nr. of blind nodes) implies that the network load should not increase too strongly when a blind node is added to an AME ZigBee network. Table 1 includes the network load. A single star ($\star$) indicates that blind nodes can operate in the passive configuration, which minimizes network load. A double star ($\star\star$) indicates the that there is more network load caused by two-way communication between a blind node and reference nodes. This means that ToF based methods are ruled out.

Note that Requirement 5 (Enhancements for specific location) is assumed to hold for each localization technique considered, because enhancements can be seen as post processing. Namely, detection of hot-spot tracking or detection of prescience in no-go areas is applicable after locations have been determined.

Localization techniques requiring additional hardware for reference nodes are excluded by Requirement 2 (Adoptability of existing AME ZigBee devices). This makes the choice for the localization technique more easy. Either ranging using RSS or fingerprinting using RSS meet the requirements. The advantage of ranging using RSS would be that there is no *a priori* phase. However, it requires knowledge of the location of the reference nodes, but the fingerprinting database needs to be known. Seems similar. A detailed literature study concerning localization techniques in WSN can be found in [5], which was written during the preceding phase of this thesis. Note that RSS fingerprinting was not included in that document.

Up to here, both ranging using RSS and fingerprinting using RSS are possible solutions for solving the indoor localization problem. In order to choose between them, Chapter 3 analyzes signal transmit power.

3 Signal Transmit Power

From the survey of localization techniques in WSN described in Chapter 2, signal strength is a preferred metric for a solution of the localization system developed in this thesis. There are two ways described to use signal power in localization. Either as a range method where distances between ZigBee devices are estimated in order to use multilateration for localization, or as a range free method in the sense of fingerprinting.

A ZigBee radio is able to send and receive radio waves in the $2.4Ghz$ frequency range. A radio can generate an electromagnetic wave with a certain power. Signal power reduces when the wave propagates through air or other matter.

The remainder of this section goes into the theoretical model of signal power. The correlation between signal power and distance is explored. It comes out that the model does not apply in practice. When the correlation between signal power and 2D surface is explored, it comes out that a fingerprinting technique is the right possible solution to the problem defined in Chapter 1.

3.1 Model

Usually in scientific research, a good model contributes to a good insight in the problem. The model described in this section is a first order representation of radio signal propagation. It does not take reflections and isotropy into account. An isotropic antenna broadcasts power equally in all directions.

If a radio signal propagates the absolute path from sender S to receiver R, as depicted by Figure 6, then the following theory applies.

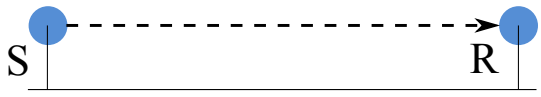

Figure 6: Radio propagation.

The correlation between signal power RSS and distance d is defined by [1] in Equation 3.

$$RSS(d) = -(10n \cdot \log_{10} d + A) \tag{3}$$

In this equation, parameter A represents the RSS value measured at $1m$ from the sender. Parameter n represents an environment constant and depends on matter of propagation and obstructions. Both A and n can be determined experimentally. A can be determined

by measuring the signal power at one meter distance from the sender. Knowing A, n can be determined using Equation 3. A graphical representation of the inverse function is given by Figure 7.

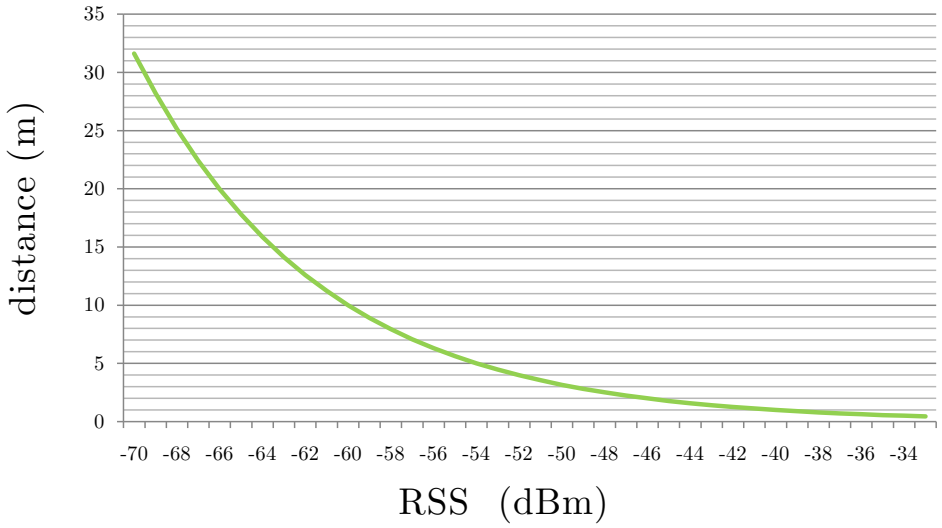

Figure 7: RSS versus distance, where $n = 2$ and $A = -40$.

Because of the logarithmic component in Equation 3, variance in an RSS measurement gives more inaccurate distances for lower RSS values. Namely, the flatter the curve the more accurate the distance estimation. This means that higher RSS values are more accurate than lower RSS values, and thus closer distances are more accurate.

3.2 Practice Compared to Model

In order to verify if the model described in the previous section applies to practice, experiments have been executed. The equipment for the experiments is described below. The first experiment verifies if the signal power to distance mapping can be used for distance estimation. The goal of the second experiment is to determine to what extend the AME ZigBee product called "Circle" is isotropic.

The experiments were done in an outdoor environment at an open football field. This is because a football field is an open site, without any possible disturbances of other radio transmitters. It turned out that a football field is not a non-reflective site, as described in the following sections.

The vendor of ZigBee IC's Ember (`www.ember.com`) offers an implementation of the ZigBee stack. Ember's ZigBee stack includes a signal strength measurement. Ember defines the

Received Signal Strength Indicator (RSSI) to be the value representing the energy level in dBm at the radio's receiver; "The RSSI measurement is based on the peak (highest) energy level detected by the radio on the current frequency over the first eight symbol periods (about 128 μs) of the current packet being received". For experimental usage, *ping* messages are used. A ping message is a basic message in the application layer, containing no data or payload. A ping message can be used to request or advertise presence information.

In the remainder of this document, the RSSI measurement supported by the Ember stack will be denoted as RSS measurement.

3.2.1 Equipment

The experiments have been done using the following equipment.

(a) Circle (b) Stick

Figure 8: Examples of AME ZigBee products.

A Circle (Figure 8a) is an AME ZigBee device which can be placed in a wall socket to measure and communicate power consumption. Circle devices are used as reference nodes. A Stick (Figure 8b) is an AME ZigBee device which can communicate Circle's measurement data to a Personal Computer.

The measurements described in the following sections are done using one Circle and one Stick. The Circle devices are intended for use as reference node. The Circle was configured to send ping messages. The Stick was configured to measure signal strength of received ping messages coming from the Circle. The RSS values are sent via serial communication to a notebook PC, which is able to record incoming messages. Since only two devices were used, routing was disabled. The disabling of routing is important since RSS measurements are done on the last hop of transmission.

3.2.2 Isotropy

The goal of the isotropy experiment is to analyse to what extend the orientation of a Circle influences an RSS measurement, i.e. the uniformity of power in all directions. The isotropy model has been extracted by means of measurements in all spatial dimensions (x, y, z). Ideally, the ZigBee device distributes its power uniformly in all directions.

Figure 9: Dimensions of a Circle.

Both Circle and Stick were placed at the same height of $0.5m$, just as illustrated by Figure 6. At a distance of $1m$, the RSS measurements of ZigBee packets coming from the Circle were done by the Stick. In each of the three dimensions, the Stick performed RSS measurements at twelve positions. At least 200 RSS measurements have been done at each position. In 36 measurement positions, the Stick was placed orthogonal to the Circle.

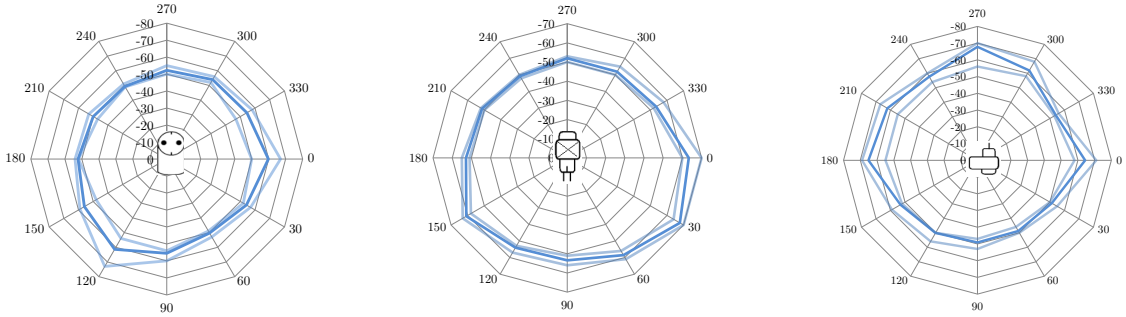

(a) XZ pane (b) XY pane (c) ZY pane

Figure 10: Received Signal Strength at $1m$. Angle in degrees.

The light blue lines indicate minimum and maximum RSS measured at the corresponding position. The average RSS measured is indicated by the dark blue line. It is easy to see that the power distribution of the Circle is not uniform in all directions. The variance in the RSS measurements is up to $20dBm$, which already indicates that distance mapping

from RSS measurement is hard. The variance is seen as noise in the measurement, since all other factors are constant.

When a Circle is mounted in a wall socket, then the part of Circle which is "seen" has relative low variance of $3dBm$. The part of a Circle which is seen when mounted in a wall socket is clockwise from 0° to 180° in the XY pane Figure 10b), and clockwise from 180° to 0° in the ZY pane (Figure 10c). However, the targeted localization scenario is when a blind node does an RSS measurement on a message received from an arbitrary Circle; the blind node does not know the orientation of the Circle with respect to his own position. This means that although the isotropic graphs of Figure 10 look good from a sight perspective, the orientation does influence the RSS measurement.

Based on the isotropy model extracted from a Circle, it can be stated that RSS values are orientation dependent and have an average spread of $6dBm$. This implies that orientation should be taken into account, when an RSS measurement is done.

3.2.3 1 Dimension (Distance Correlation)

In order to verify the RSS versus distance correlation defined by Equation 3, the following experiment has been executed at a football field. RSS measurements have been done using the setup as used in the isotropy experiment, at a distance ranging from $0m$ up to $20m$. The orientation of the Circle with respect to the Stick was at a position of 90° in the ZY pane. The Stick was orthogonal oriented with respect to the Circle.

At a resolution of $1m$, the measurements were performed. Just as in the isotropy experiment, at least 200 RSS measurements were done at each of the 21 locations. The result of the extracted signal power to distance correlation is compared to the theoretical correlation in Figure 11.

The average of the RSS measurements is plotted and compared to the theoretical curve. Note that Figure 11 has reversed axes compared to Figure 7. This is because the red graph is not injective, since it has multiple distances for particular RSS values. For example, an RSS value of -68dBm maps to $7m$ and $9m$.

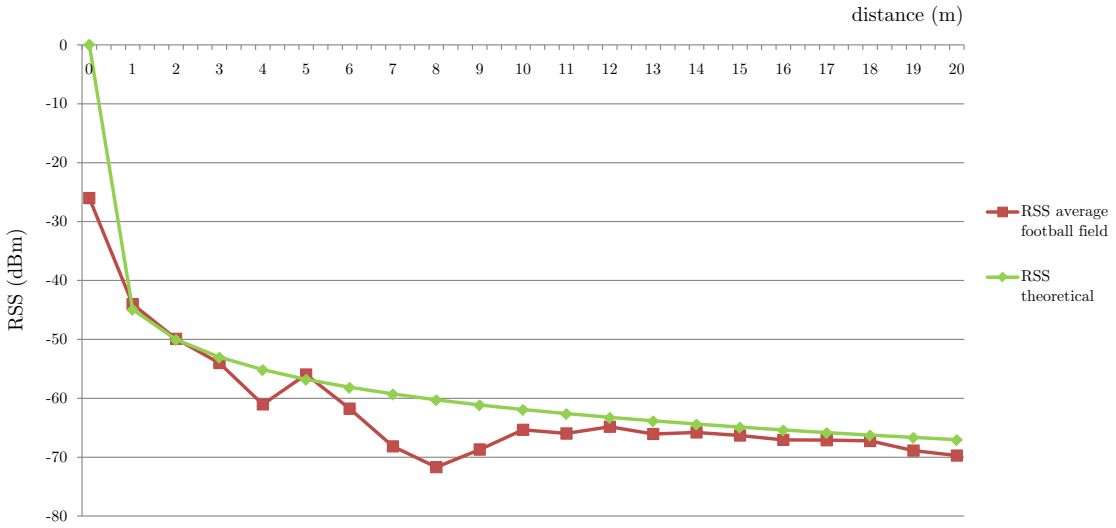

Figure 11: RSS measurements at football and theoretical model

Unfortunately, the RSS does not correlate with distance as the theoretical curve. Moreover, the correlation between RSS and distance is not injective in practice. It can be concluded that a higher RSS value gives rise to a closer distance, as the theoretical model of Section 3.1 describes. The steep part of the graph (RSS values $>$ -52dBm) is injective, and enhancements have been tried to spread this steep part, in order to achieve an injective function. This has been done by increasing the output power of the Circle, using different antennas for the Stick averaging RSS values from multiple Stick's and using different orientations of the Stick [5].

Since the relation between RSS and distance is not injective, it is not possible to determine an accurate distance based on an RSS measurement.

To understand why practice does not meet theory, reflection is added to the model.

Reflection
Since a 1 dimensional experiment is done with the Circle and the Stick in an open field, the model shown in Figure 12 would apply. Reflection via ground is added to the model. The left blue dot represents the Circle, whereas the right blue dot represents the Stick. Over the air communication is reflected via the ground. It is assumed that all other reflections do not end up at the blind node.

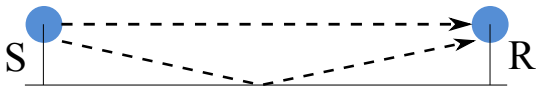

Figure 12: Reflection via ground.

The height of Circle and Stickwas equal and constant. The distance between reference and blind node was varying over the x-axis. It is assumed that there is only one reflected signal

in an ideal situation. The absolute difference between the length of the direct signal and the length of reflected signal z can be defined as follows.

$$\Delta = 2 \cdot \sqrt{h^2 + \left(\frac{x}{2}\right)^2} - x\,\mathrm{m} \tag{4}$$

Then, we determine the wavelength by the following formula.

$$\lambda = \frac{v}{f} = \frac{299.792.458 m/s}{2.4 Ghz} = 0.125\,\mathrm{m} \tag{5}$$

Then, the difference between x and z in terms of lambda is formulated by the following.

$$\Delta_\lambda = \frac{\Delta}{\lambda} \tag{6}$$

This difference in terms of lambda is related to the attenuation of signal strength measured at the blind node. Namely, the attenuation factor is defined as follows.

$$k = \cos(2\pi \cdot \Delta_\lambda) \tag{7}$$

This attenuation factor applies to the power measured at the receiving node. Therefore, the measured signal power in dBm is transformed into power in Watt by the following formula.

$$P = 10^{\frac{(x-30)}{10}} \tag{8}$$

Where x is the power in dBm, and P the power in W.

Thus, the theoretical and practicable correlation between RSS and distance are transformed to lineair power, and multiplied by the attenuation factor. This results in the following graph, knowing that the height was $0.5m$.

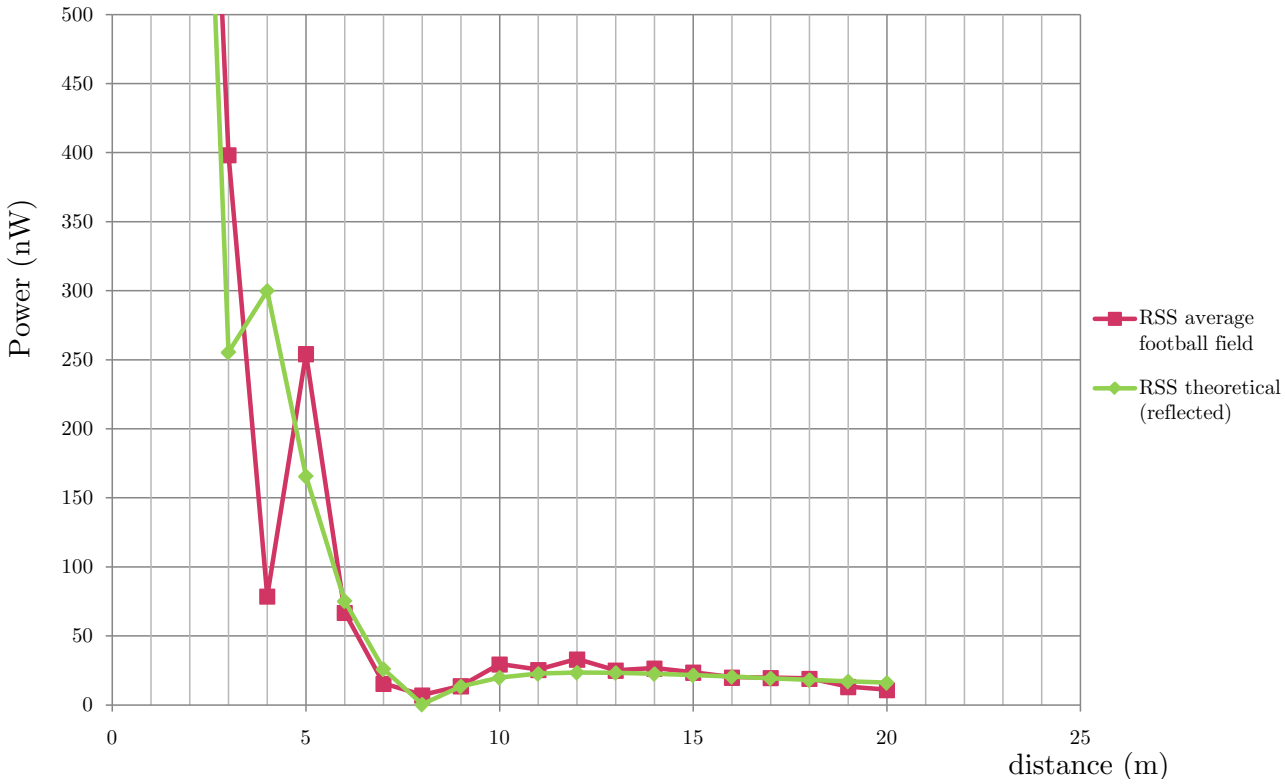

Figure 13: Reflection theory.

The green line denotes the theoretical power in nW with attenuation from the modeled reflection signal. The red line represents the measured power in nW from the 1 dimensional distance experiment.

In the initial distance experiment the football field was chosen to be the site for the experiment. It was thought that the football field was a "clear" site without disturbances. However, it is proved that the reflection via the ground is there, which makes the RSS to distance mapping to be no longer injective. This means that a particular RSS value can be mapped to multiple distances. This disables the possibility for distance determination using RSS. This implies that the range method using multilateration based on RSS cannot be applied.

3.2.4 2 Dimensional

From the previous section it is known that the measured received signal strength is influenced by reflections via ground. This disables the possibility to map RSS measurements to

distances, thus multilateration using RSS measurements cannot be a solution tot the localization problem. Moreover, the reflection theory described in the previous section does not include reflections ceiling, walls, closets and other obstacles in an indoor environment.

Still we continue exploring to a RSS based localization scheme. The exploration is done under the assumption that reflections are static. By static is meant that if an RSS measurement is done at two movements in time, then it is expected that the measurements results are equal.

The assumption that RSS measurements are static in time is verified by a simple experiment. This verification is done as follows. The experiment verifying the RSS to distance correlation (Section 3.2.3) is done twice. If both experiments give equal results, then the assumption holds. The result is shown in Figure 14.

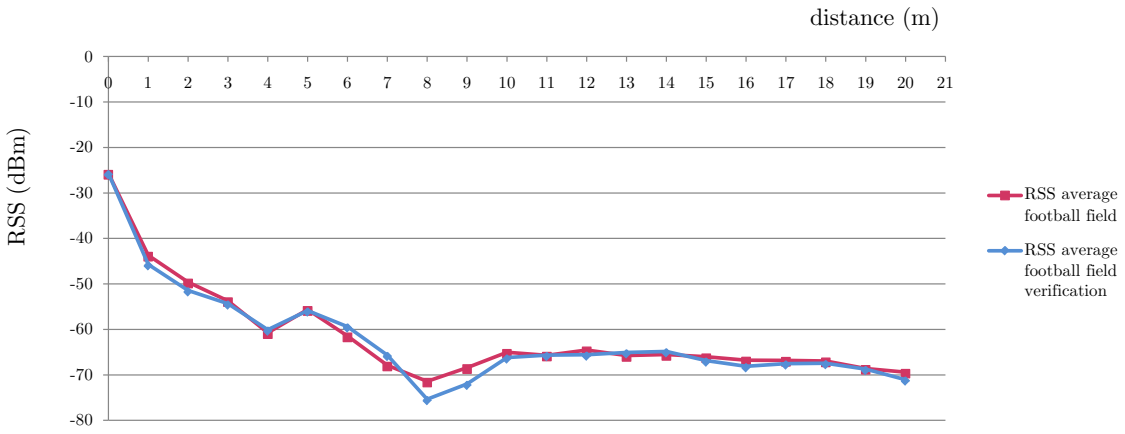

Figure 14: Verification if RSS measurements are static in time.

The plot shows two experiments. Experiment 1 is equal to the RSS-at-football-field graph from Figure 11. Experiment 2 is executed exactly equal to Experiment 1. We can see that both graphs follow the same curve, except from $7m$ to $10m$. Indeed, $8m$ is exactly the distance where the attenuation is the strongest according to Figure 13. Difference in the experiment results from $7m$ to $10m$ can be explained by the fact that attenuation is very local, which means that little variance in position of measurement causes relative high variance in RSS measurement. Since positioning of the measurement device (Stick) is done by hand and using a tapeline, the chances are that there is little variance in positioning in comparison to the first experiment. Therefore we conclude that the RSS measurements are static in time.

Knowing that RSS measurements are static in time, an RSS value can be compared to a predefined value in order to scat possible locations. Therefore an investigation has

been done to extract RSS measurements at different locations in AME's warehouse. The warehouse contains metal racks accommodating electronic related supplies. Because of the racks, ceiling and ground, and other obstructions; there are a lot of reflections. The dimensions of the warehouse are $29m$ x $30m$ x $4m$. One Circle is mounted at position ($6.3m$, $5.2m$), at a height of $2.9m$. Following the model of previous section (Equation 3), the theoretically expected RSS value at each position in the warehouse is calculated. The set of expected RSS values for each position is called a *signal map*. A plot of the theoretical signal map is shown in Figure 15. Note that for ease of interpretation of the Figure, the RSS values are all increased by 100. For generation of Figure 15, Equation 3 has been used substituting $n = 1.3$ and $A = -52$. These values for n and A have been determined experientially using the same method as the 1D experiment, but performed indoors.

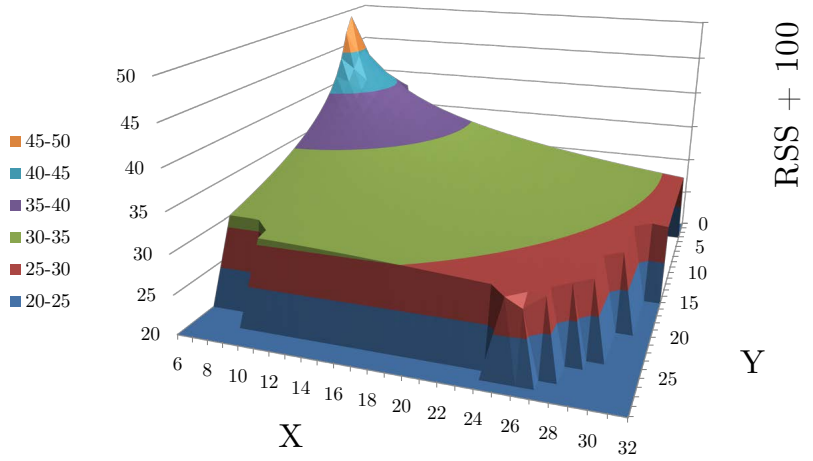

Figure 15: Theoretical Received Signal Strength + 100 of a Circle placed at ($6.3m$, $5.2m$) at a height of $2.9m$.

In the following, this 2D model is compared to practice. Since it is requires too much time to sample RSS measurements at each position in the warehouse, interpolation has been applied. The interpolation method is described in Chapter 4.

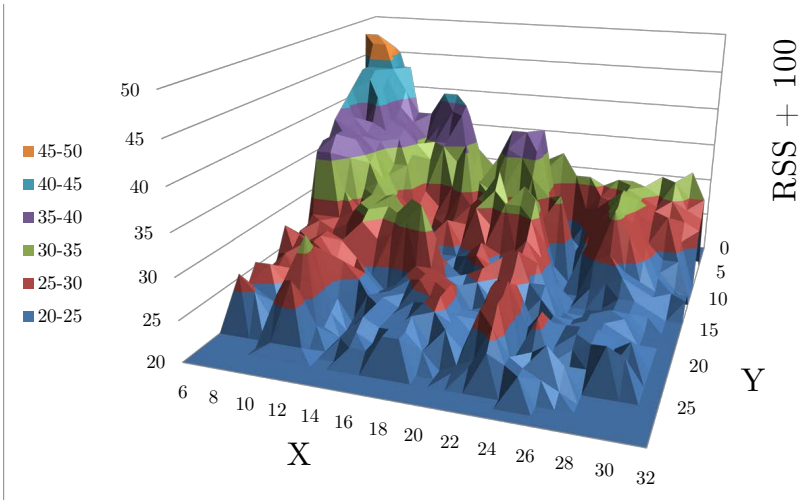

Figure 16: Measured Received Signal Strength of a Circle placed at (6.3m, 5.2m) at a height of 2.9m.

Comparing theory to practice (i.e. comparing Figure 15 to Figure 16), we can see that in practice the function of RSS is not a monotonic. It is very likely that the non-monotony is because of reflections and not always having LoS between Circle and Stick. We can also see in practice, that the RSS values can be either higher or lower than expected by the theoretical model. This is because reflections can attenuate the RSS measurement, but reflections can also strength the RSS measurement. Namely, strengthening can be occur if the signal paths arrive equally phased.

3.3 Conclusion

In order to come up with a solution to the localization problem, RSS seems to be a preferred metric as concluded in Chapter 2. It is shown that orientation of a Circle influences the RSS measurement, since a Circle does distribute its signal power equal in all three dimensions. This means that RSS measurement of signals coming from a Circle should take orientation into account.

Secondly, from Chapter 2 we know that RSS can be used in either a range or range free fashion. In practice, RSS cannot be used as a range method since reflections cause signals to be received from multiple paths. This results in an injective RSS to distance mapping, which disables clear distance calculation based on RSS. The reflection theory has been verified in outdoor experiments. However, it is shown that RSS measurements are static in time.

The static nature of RSS measurements can be used for comparison to a predefined value. The next section proposes a localization scheme based on stateliness of RSS measurements.

4 Localization Scheme

Based on our claim that RSS measurements are static in time, this thesis proposes a training based localization system. Training based localization consists of two phases, a *training phase* and a *localization phase*. A training phase is done before the actual localization is done. The first phase, the training phase, results in a database containing signal maps for each reference node. In the second phase, the localization phase, the "live" fingerprint, containing RSS measurements from neighboring nodes, is compared to the fingerprints in the database in order to determine a location.

Training based localization requires undesired *a priori* work. Namely, before localization can happen the *a priori* training phase must be done. This is undesired since it makes the installation of the localization system take more time. On the other hand, a training based localization scheme does not require knowledge of the position of reference nodes while range localization methods do. Thus, considering Requirement 2 (Adoptability of existing AME ZigBee devices), the engineer installing the localization system at a site does not have to care about exact positions of reference nodes, as long as they are roughly equally distributed along the localization area. Since most AME ZigBee networks are typically roughly equally distributed Circles, they are suitable for use as reference node.

Note that the signal maps described in the previous section are treated in a continuous fashion, e.g. for each location (x, y) an expected RSS value is present. In this thesis, the matching algorithms for comparing fingerprints are explained assuming that $x, y \in \mathbb{R}$. The resolution r of x and y is proportional to the database size. For example, having $r = 100cm$ enables a finite signal map for a localization area. Then each location (x, y) and its corresponding fingerprint are represented by a *tile*. A tile covers the area from (x, y) to $(x + r, y + r)$.

The remainder of this section describes the two phases of training based localization. Analysis focusses on ease of training, localization accuracy, and running time of the localization algorithm.

4.1 Training Based Localization

The training phase is schematically illustrated by Figure 17.

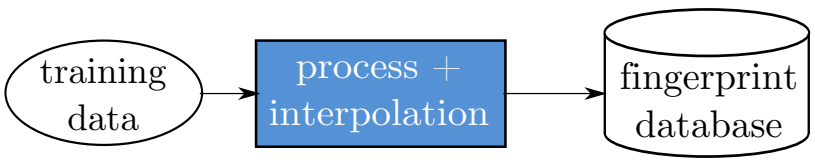

Figure 17: Training phase of training based localization.

The training is done by an installation engineer. The generation of the fingerprint database from training data is done by interpolation. The training phase results in a set of signal maps, called a fingerprint database. For recapitulation: a signal map is a set of expected RSS values for all locations in the localization area, for a given reference node. In other words, the fingerprint database contains for each location (x, y), a fingerprint $S_{x,y} = (s^1_{x,y}, s^2_{x,y}, \ldots, s^i_{x,y}, \ldots)$ where $s^i_{x,y}$ represents the expected RSS value for a reference node i.

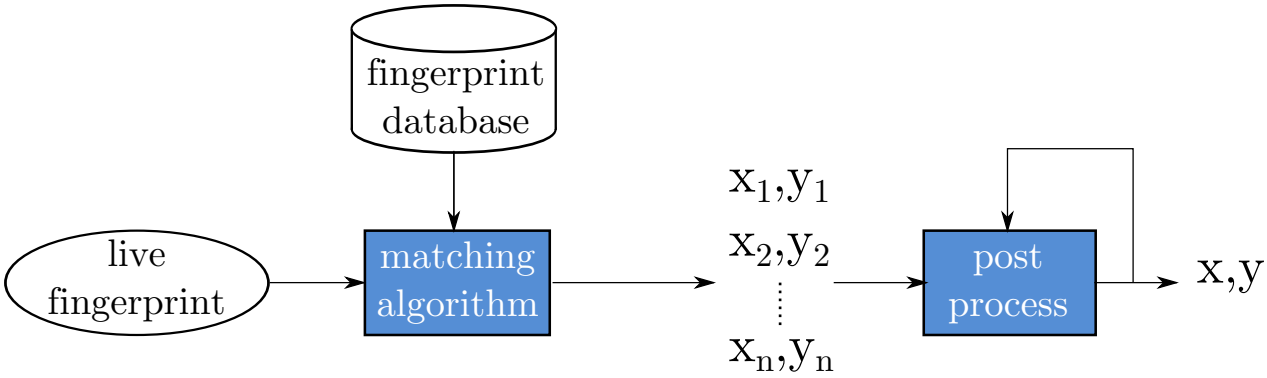

Figure 18: Localization phase of training based localization.

The fingerprint database constructed by training is used by a blind node in the localization phase as depicted in Figure 18. In the localization phase, the live fingerprint is compared to the fingerprints from the database in order to judge possible locations. Judgement is done by giving a weight to a possible location. Sorted by their weight, the top k locations form the outcome of the localization algorithm.

The postprocessing of the set of weighted locations depends on the target application. For example, a weighted average of the top k positions can be calculated, in order to come to a single location. Another possibility is that the application gives reason to limit speed. Speed limitation can be done by storing the previous localization outcomes and limit the euclidian distance of successive localization outcomes. This thesis focusses on the location calculation itself. This means that there is no focus on postprocessing. Therefore the weighted average location of the top k tiles is used.

Assumptions
For the proposed localization scheme, the following assumptions are made.

1. The position and orientation of reference nodes is equal in training phase and localization phase. Reference nodes are not moved or removed.
2. Reference nodes are roughly equally distributed along the localization site. Target distribution is one reference node per $70m^2$.
3. The hardware of the blind node is equal in training and localization phase.

4. Each second, a reference node sends asynchronously a beacon message at the MAC layer.
5. Only changes in furniture of the localization area are allowed. A rebuilding gives rise to a new training.

The assumptions give rise to explanation. Signal maps are generated from RSS measurement at a different moment in time than localization takes place. RSS measurements will only reproduce if the reference node is positioned at the same location and orientation (assumption 1) and the blind node is equal in terms of hardware (assumption 3). It is assumed that the density of reference nodes is at least one reference node per $70m^2$, as is in AME's building. In order to enable RSS measurements, a reference node sends periodically a beacon message (assumption 4). A beacon message is a 1-hop message only received by a neighboring Ember ZigBee device if it is configured to receive it. By neighboring, the area of direct communication is meant. We have tried to send beacon messages at the application layer, but this results in overflowing buffers of reference nodes, which is prohibited by Requirement 2 (Adoptability of existing AME ZigBee devices).

Changes in the localization site can affect signal power distribution of reference nodes. Therefore only changes in the furniture of the localization area are allowed; otherwise the RSS measurements will not reproduce. In practice, this means that a rebuilding gives rise to do a new training, as is explained in Section 5.2. Namely, a rebuilding means that the reflections in a building are heavily changed which causes different signal power distribution of a reference node. Note that only one assumption has been made about the environment, fulfilling Requirement 4 (Blind node has no environmental knowledge).

4.2 Training Phase

The goal of the training phase is to construct a fingerprint database, which can be used during localization. This section describes how the fingerprint database is constructed out of training data.

A fingerprint database consists of signal maps. As Requirement 4 (Blind node has no environmental knowledge) states, the installation of the localization system is intended to at most one day. Therefore a relatively low-time-consuming training phase is proposed, where not all locations of the localization site are physically visited.

The fingerprint database to construct can be built by either calculating the signal maps [3], or by extraction while physically visiting parts of the localization area. The drawback of calculating signal maps is that the location, orientation and reflections need to be taken into account. The model for calculation becomes complex. Therefore this thesis proposes a novel training. Since the goal of the accuracy of the proposed system is room-level accuracy, only the contours of the loculation site must be physically visited. The advantage of visiting

the contours is that each room is treated separately, as will be explained in the remainder of this section.

An installation engineer is visiting the contours, while carrying one or more blind nodes. Visiting the contours, the blind nodes send all their RSS measurements to a PC. Because of assumption 4, reference nodes are autonomously sending beacon messages, which enables a blind node to perform RSS measurements from beacons received from neighboring reference nodes. When all contours are visited, the interpolation of RSS measurements to signal maps is calculated by the PC.

For the remainder of this section, it is assumed that walking contours is done by straight tracks. This is for ease of explanation. Furthermore, the manner of building a signal map from training data is explained for one single reference node.

The explanation of the training phase goes by a small fictive office localization site, see Figure 19.

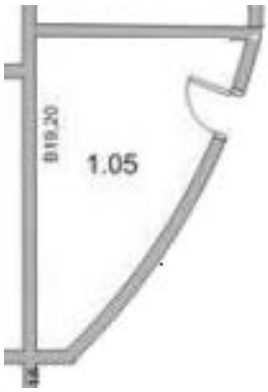

Figure 19: An example of a localization area.

In this case, the contours of the office are walked in five tracks, represented by blue straight lines in Figure 20a. While walking these tracks, RSS measurements done by the blind node are sent to a PC and stored on hard disk. The mapping of RSS measurements to a location on the map is done linearly in time, see Figure 20b. For each track the start and end location is known. In practice, this can for example be done by the installation engineer by clicking on a map using a PC application.

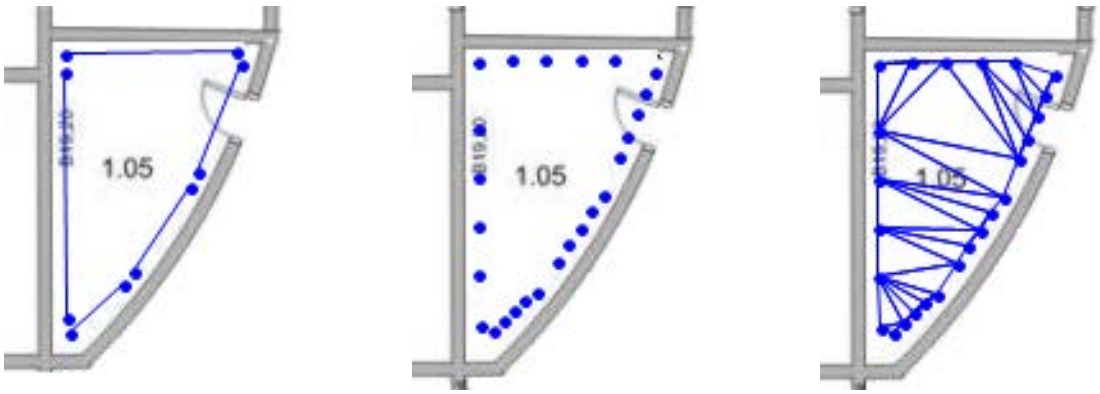

(a) tracks walked (b) RSS measurements mapped to locations (c) positions triangulated

Figure 20: Interpolation steps.

The third step is to interpolate the RSS measurements. Because a triangle is one of the basic shapes in geometry, we have chosen to interpolate RSS measurements using the closest three training RSS measurements. This is achieved using *Delaunay* triangulation [11]. Delaunay triangulation is a useful technique for quickly generating non-overlapping triangular meshes that reflect the nearest neighbor.

In order to construct a signal map, we must have a generic method to compute an RSS value for a given location. Whenever we want to interpolate an RSS value at a given position, we just lookup the circumscribed triangle. Then, the Barycentric coordinates of the triangle are used to compute the interpolated RSS value [11]. The Barycentric coordinate system specifies vertices of multidimensional triangles. Besides x and y, our third dimension is RSS.

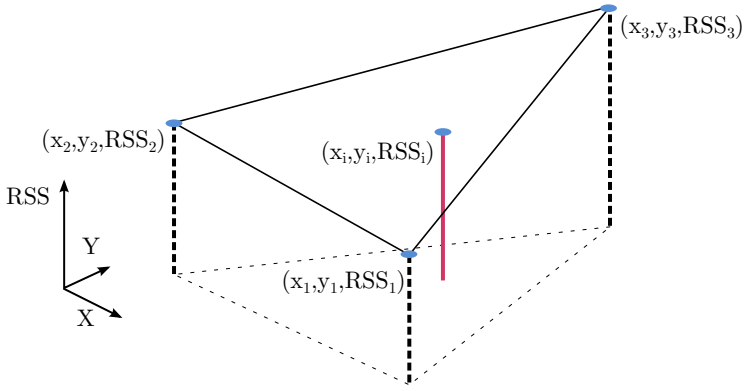

Figure 21: Interpolation is done using Barycentric coordinates.

A triangle with Barycentric coordinates $(x_1, y_1, RSS_1), (x_2, y_2, RSS_2), (x_3, y_3, RSS_3)$ is shown in Figure 21. The coordinates of the triangle are RSS measurements from training tracks,

just as in Figure 20c. Compared to Figure 20c, Figure 21 adds the RSS dimension. To compute the interpolated RSS value at the location (x_i, y_i) indicated by the red line, we compute [11]:

$$b = (x_2 - x_1) \cdot (y_3 - y_1) - (x_3 - x_1) \cdot (y_2 - y_1) \tag{9}$$

$$b_1 = \frac{(x_2 - x_i) \cdot (y_3 - y_i) - (x_3 - x_i) \cdot (y_2 - y_i)}{b} \tag{10}$$

$$b_2 = \frac{(x_3 - x_i) \cdot (y_1 - y_i) - (x_1 - x_i) \cdot (y_3 - y_i)}{b} \tag{11}$$

$$b_3 = \frac{(x_1 - x_i) \cdot (y_2 - y_i) - (x_2 - x_i) \cdot (y_1 - y_i)}{b} \tag{12}$$

Substituting the coordinates of the triangle in Equations 9, 10 and 11 we compute the contribution of each RSS measurement (vertex of the triangle) according to euclidian distance in x and y dimension. Then, an interpolated RSS value can be computed using Equation 13.

$$RSS_i = RSS_1 \cdot b_1 + RSS_2 \cdot b_2 + RSS_3 \cdot b_3 \tag{13}$$

Note that this interpolation technique only applies to locations that fall inside a triangle. This means that locations outside the enclosing polygon of the RSS measurements (see Figure 20c) cannot be interpolated.

4.2.1 Non overlapping signal maps

All RSS measurements from any reference node done during a training track are mapped to a location in the localization area. The set of RSS measurements of different references nodes typically have different enclosing polygons, which results in not entirely overlapping signal maps of reference nodes. For ease of explanation there are only two reference nodes considered, let's say the green and red reference node. Let us consider a fictive rectangular localization area as depicted by the circumscribed square in Figure 22.

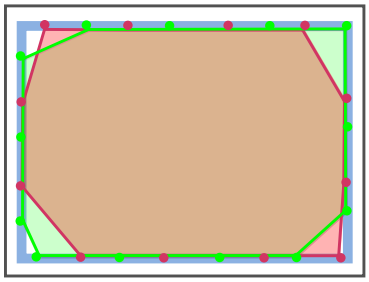

Figure 22: The covered area of signal maps are not entirely overlapping.

The training tracks walked are represented by the four blue lines forming a rectangle. A dot represents an RSS measurement performed during the walk of the corresponding track. The color of the dot identifies the reference node of the RSS measurement. The enclosing polygon of the dots of a color represent the covered area of the signal map of a reference node. As one can see, the red and green polygons do not entirely overlap. This is due to mapping of RSS measurements to a location. The mapping depends on the time of arrival of the beacon message, which is sent asynchronously. Thus RSS measurements are individually mapped to a unique location. Having non overlapping signal maps means that there are locations where there is an expected RSS value for the red node but not for the green node and vice versa.

Moreover in a real situation, it can be that there is only one expected RSS value at a given location. Having only one expected RSS value at a location is too little, because some comparison algorithms favor locations with few expected RSS values over locations with more expecters RSS values. An example is the RADAR localization matching algorithm, as will be explained in Section 4.3.1. We cannot just take the intersection of the enclosing polygons, since an individual reference node does not cover the whole localization area; this would imply that the intersection can be $\emptyset$. To solve the problem of non-overlapping signal maps, we have chosen to have a minimum m of expected RSS values for a fingerprint. This means that for every fingerprint in the fingerprint database, we have at least m expected RSS values. Fingerprints having less than m expected RSS values are not contained in the fingerprint database.

4.2.2 Averaging out errors

We know RSS measurements are theoretically static in time. However, in practice there is variance in RSS measurements as we have seen in the experiments from Chapter 3. The fingerprint database should contain an average RSS value in order to represent the most likely expected value for an RSS measurement.

Therefore, a multiple of k blind nodes can be used during training. For each reference node, the interpolation should then be executed for each of the k blind nodes. The average of the outcome of the interpolation executions should be contained in the signal map of the reference node. We experienced that $k = 3$ is sufficient, as will be explained in Section 5.1.

4.2.3 Conclusion

From Chapter 3 we know that for RSS measurements, the orientation of the sender should be taken into account. This is implicitly done by the proposed training phase. Namely during training, at different locations RSS measurements are performed at different orientations of the reference node with respect to the blind node. To conclude, the training tracks walked are used to linearly map RSS measurements to locations in the localization site. The positions of these RSS measurements are triangulated using Delaunay triangulation. Using Barycentric coordinates with x, y, and RSS dimensions; at each position (x, y) in the enclosing polygon we can compute an interpolated RSS value for a given reference node. This interpolated RSS value is the expected RSS value for the given reference node. Using this interpolation, the signal maps for the reference nodes are built. A better fingerprint database can be build using multiple blind nodes during training. The problem of non-overlapping signal maps can be solved by using a minimum number of RSS values in each fingerprint in the database.

4.3 Localization phase

The actual localization is described in this section. In the localization scheme proposed, the live RSS measurements are combined to a fingerprint. This live fingerprint is compared to the database using an matching algorithm, see Figure 23. The result of the matching is list of weighted possible tiles. Postprocessing is not described in this section, since it is out of scope of the localization phase. The remainder of this section compares two matching algorithms known from literature. The comparison focusses on localization accuracy and running time.

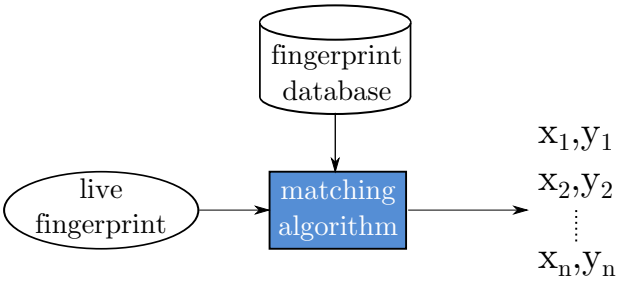

Figure 23: Localization phase without post processing.

Most of the matching algorithms known from literature assume that there is a fingerprint database containing a fingerprint for each tile in the localization site, as this thesis also does. Other matching algorithms assume only individual fingerprints for specific locations in the localization area (thus without interpolating RSS values for all tiles). The matching algorithms known from literature are listed.

RADAR The RADAR matching algorithm is a basic matching algorithm that judges the likelihood of possible tiles based on nearest neighbor matching in signal space [2]. RADAR is known as the foundation of fingerprinting localization.

ABP The Area Based Probability (ABP) algorithm estimates statistical maximum likelihood [6].

SPM Single Point Matching (SPM) uses threshold bounding of fingerprints [6].

In [8], *Kleisouris et al.* show an experimental algorithm survey including all three localization algorithms RADAR, ABP, and SPM. For ABP and SPM signal maps were used, as this thesis also does. For RADAR they used a set of training points, which is a subset of a signal map. Their experimental setup also differs from the proposed system of this thesis. Namely, they used a blind node in an active manner (as explained in Chapter 2). This means that one beacon message sent results in a number of RSS measurements, whereas in our case one beacon message sent results in one RSS measurement. The authors used the single top tiles from the algorithms outcome.

The accuracy of a localization system is usually expressed in a Cumulative Distribution Function (CDF). A CDF shows the cumulative probability of the localization error. The localization error is defined to be the euclidian distance in two dimensions ($E = \sqrt{(x - x_{real})^2 + (y - y_{real})^2}$). A CDF can be seen as the "error so far" function of the probability distribution. *Kleisouris et al.* show that usage of multiple antennas at the reference nodes can increase the localization accuracy, as depicted by the CDF of the localization accuracy in Figure 24. Note that since the authors used active blind nodes, their reference nodes are equipped with multiple antennas, in contrast to our passive blind nodes. This is a major difference compared to our solution, but we think having multiple antennas is worth analyzing.

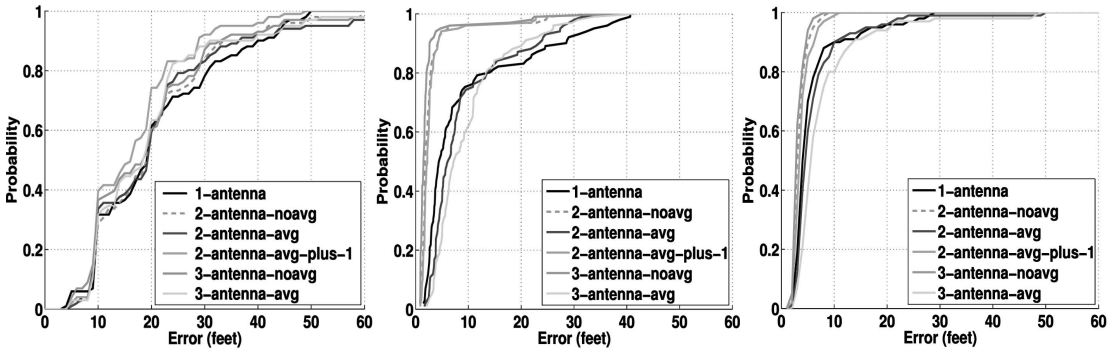

(a) RADAR (b) ABP (c) SPM

Figure 24: CDFs for localization in WSN [8].

The authors considered six antenna configurations. The configurations differ in the amount of antennas of reference nodes taken into account, and the way the different antennas are combined. Namely, combining can be done by either averaging RSS values for a reference node or having a separate signal map per antenna of a reference node.

This thesis only considers the *1-antenna*, *2-antenna*, and *3-antenna* configuration (respectively comparable to *1-antenna*, *2-antenna-avg* and *3-antenna-avg* in Figure 24). This is because of practical reasons. The targeted hardware design for a blind node only consists one ZigBee radio. An additional PCB with another (two) ZigBee radio(s) can be mounted, but this additional PCB has not yet been designed. Besides, we consider a maximum of one fingerprint database. This is also because of practical reasons. Namely, computation power and storage space of an embedded device are limited.

Considering the single antenna configuration (e.g. *1-antenna* in Figure 24), RADAR's median localization error (probability = 0.5) is $20ft$ ($6.1m$), and the 80th percentile error of the localization has an error of $< 30ft$ ($9.1m$). In contrast to RADAR, APM and SPM perform better as can be concluded because of the steepness of Figure 24b and Figure 24c. Namely, the 50th percentile error of both ABP and SPM is $< 5ft$ ($1.5m$), and the 80th percentile error is $< 15ft$ ($4.6m$) and $< 7ft$ ($2.1m$) respectively. SPM seems to perform

the best among the three algorithms. Also, when averaging RSS measurements from two (*2-antenna-avg*) or three antennas (*3-antenna-avg*), SPM performs the best.

Because RADAR is the foundation fingerprint matching algorithm and SPM is the best performing algorithm according to *Kleisouris et al.*, both algorithms are chosen for further analysis in this section.

4.3.1 RADAR

The RADAR method used for this thesis is known as *Gridded RADAR*[6]. Gridded RADAR assumes that there is an interpolated signal map for each reference node. Other fashions of RADAR assume for example a small set of training points instead of an interpolated signal map, as *Kleisouris et al.* do. The fingerprint matching algorithm RADAR originally comes from *Bahl and Padmanabhan* in [2]. The basic concept of the original RADAR algorithm is that it searches for the fingerprint with the smallest euclidian distance in n-dimensional space, where n is the number of reference nodes. That is, it views a fingerprint from the database as points in n-dimensional space, where each reference node forms a dimension.

For a live fingerprint $S = (s^1, s^2, \ldots, s^i, ...)$ containing live RSS measurements, the euclidian distance $E_{x,y}$ to a fingerprint $F_{x,y} = (f^1_{x,y}, f^2_{x,y}, \ldots, f^i_{x,y}, \ldots)$ can be calculated using Equation 14.

$$E_{x,y} = \sqrt{(f^1_{x,y} - s^1)^2 + (f^2_{x,y} - s^2)^2 + \cdots + (f^n_{x,y} - s^n)^2} \tag{14}$$

For each fingerprint in the database, RADAR calculates $E_{x,y}$. The tiles of the fingerprints with the least euclidian distance are returned by the algorithm. This means that if a fingerprints in the database with less expected RSS values are favored, since there are less dimensions which can increase the $E_{x,y}$.

Optional penalties can be given to missing RSS measurements in the measured fingerprint. For example, missing RSS measurements in the live fingerprint can be replaced by a predefined value.

The running time of RADAR is proportional to the size of the database, since it only iterates once through the fingerprint database. We experienced that the AME Sensor Nodecan iterate through our database in les than $1.25sec$, having 10000 fingerprints with 30 expected RSS values. Although the localization accuracy experienced by *Kleisouris et al.* is not as desired, RADAR still remains a contender for further use in this thesis.

4.3.2 SPM

SPM also utilizes signal maps. The strategy behind SPM is to find a set of tiles that fall within a threshold (or *match*) of the live RSS measurement. This is done for each reference node independently. Then the intersection I of the reference nodes sets is returned. Thus SPM first creates n sets of tiles (one for each reference node). The matching tiles for a reference node i are found by adding an expected "noise", δ, to the expected RSS value $s^i_{x,y}$ (at a tile x, y) and then returning all tiles of fingerprints that fall within the expected threshold $s^i_{x,y} \pm \delta$. SPM then determines I. If $I = \emptyset$, then SPM is redone with an increased δ; otherwise I is returned. The weight of returned tiles is inversely proportional to δ.

Because SPM is a recursive algorithm, it iterates at least once through the database. If a certain δ does not give a localization outcome, the next iteration starts. Theoretically, this can repeat until infinity. Limiting the number of recursive calls, creates the risk that the algorithm does not produce a localization outcome. However, SPM's localization accuracy as shown in Figure 24c looks promising. Therefore SPM is also still a contender for further use in this thesis.

4.3.3 Conclusion

Comparing RADAR and SPM based on localization accuracy, SPM outperforms RADAR. However, the risk of SPM is that it does not give a localization outcome after a finite number of iterations. Another drawback of SPM is the running time which can be significantly larger than RADAR's running time. Since both algorithms have their advantages and disadvantages, there is not yet a choice made for one of them. The following chapter will analyse accuracy of RADAR and SPM.

5 Evaluation

This chapter evaluates the localization accuracy of the proposed localization scheme. The evaluation is done using a benchmark routine under different conditions. The influence of a rebuilding on signal maps has been explored.

5.1 Benchmarking

For benchmarking, training data has been collected throughout the AME building. During training the assumptions were as stated in Section 4.1. All RSS measurements were collected carrying blind nodes at hip height, which was $1.10m$. The evaluation of the localization system is done offline. Several parameters of the system are investigated to verify localization error. These parameters include matching algorithm, resolution of database, offices / larger rooms, and multiradio configuration.

The following subsections describe the setup of the benchmarking and the localization accuracies in different conditions.

The RADAR algorithm used in this chapter gives a penalty to missing measurements. A missing RSS value in the live fingerprint is replaced by a value of -97dBm. For SPM, δ is chosen to grow linearly, i.e., it tries $1, 2 \ldots 10$.

5.1.1 Setup

Training tracks have been walked in order to built fingerprint databases with different resolutions. Benchmark tracks are similar to training tracks, but used for localization instead of building a fingerprint database. Both training tracks and benchmark tracks were walked using three Stick's. Each Stick was logging RSS measurements to serial output, in order to let the PC log them to harddisk.

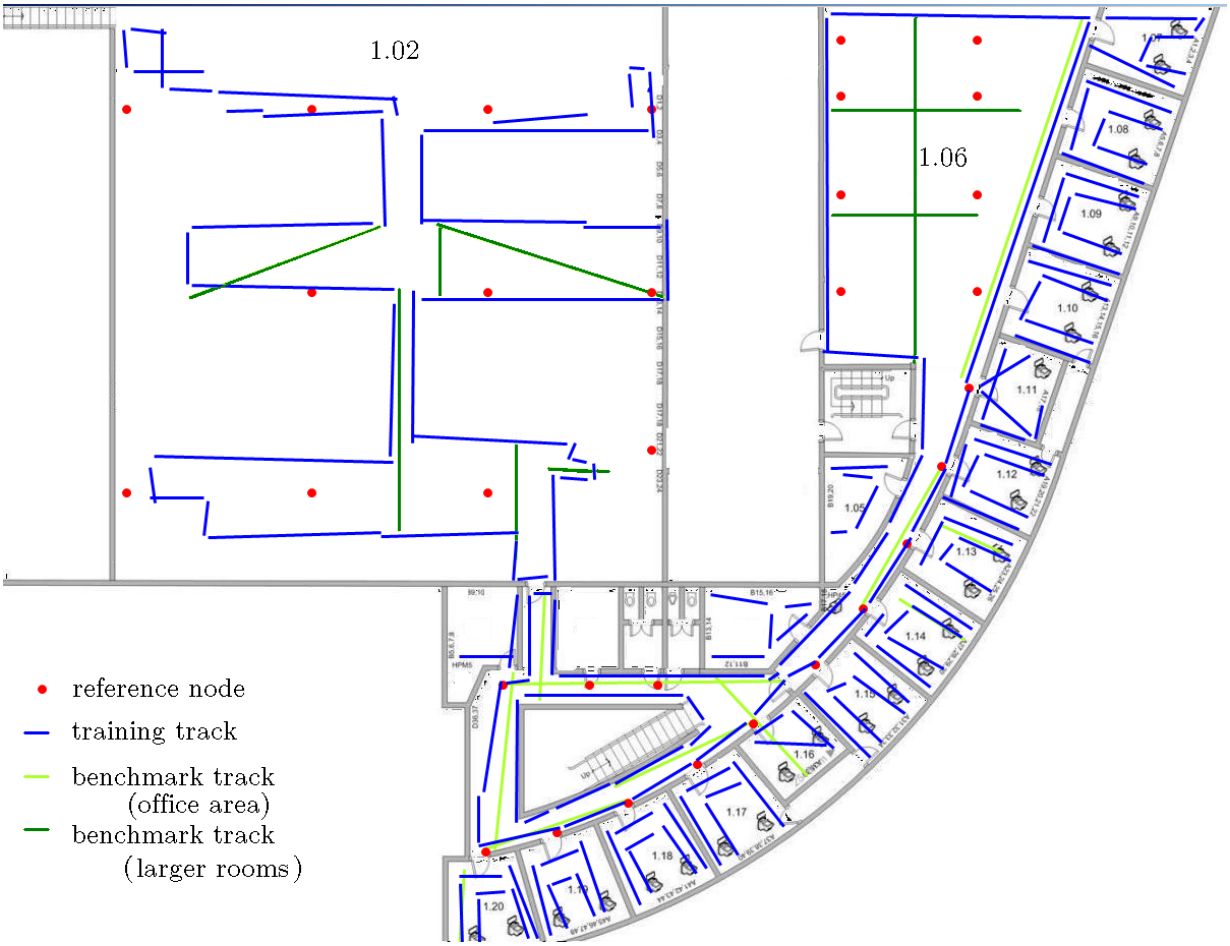

Figure 25: Training tracks walked at the first floor of AME's building.

Figure 25 shows the building plan of AME's first floor. In total 32 reference nodes are mounted above the ceiling, indicated by red dots. Training tracks walked are indicated by blue lines. As one can see, the contours of the offices along the right, the floor around the stairwell, and the canteen (room 1.06) are visited during training. The larger room in the upper left corner is trained along metal racks and a production line (both not illustrated in Figure 25).

Benchmark tracks are walked along the offices, and larger rooms 1.02 and 1.06. This is done since we think it is a good representation of the different rooms there are. The benchmark tracks are indicated by light green and dark green lines. The light green lines represent benchmark tracks along the offices. The dark green lines represent benchmark tracks for larger rooms. Benchmark tracks are stored similar to training tracks. Thus start and end location of each benchmark track is known. RSS measurements done during a benchmark track are also linearly mapped to a position and to a time, similar to reference tracks (for more information about training tracks refer to Section 4.2).

The actual benchmarking is done a benchmark routine. The parameters for the benchmark routine are the algorithm (RADAR or SPM), Δt, the multiradio configuration (*1-antenna*, *2-antenna*, or *3-antenna*), the fingerprint database and the benchmark track. For the *2-antenna* and *3-antenna* multiradio configurations, RSS measurements from multiple radios are averaged. For this survey, we choose $r = 100cm$ and $\Delta t = 2sec$. Parameter Δt represents the size of the time-window, i.e. RSS measurements falling in the window are combined to a fingerprint. The window moves over the RSS measurements of the benchmark track. The RSS measurements falling in each window are combined to a fingerprint. For each window, the real location is determined to be on the line segment between begin and end of the benchmark track. The real location is calculated proportional to the window's position with respect to length of the track. The euclidian distance in x and y dimension between the real location and the outcome the location algorithm.

We want to get a single location to determine the localization error. But, the outcome of a localization algorithm is not a single location but a set of tiles. This means we need to postprocess the set of tiles into a single location. A way to postprocess the set of tiles is to average the locations of the top k tiles. The centroids of the top k tiles returned by the algorithm are then averaged proportional to their weight.

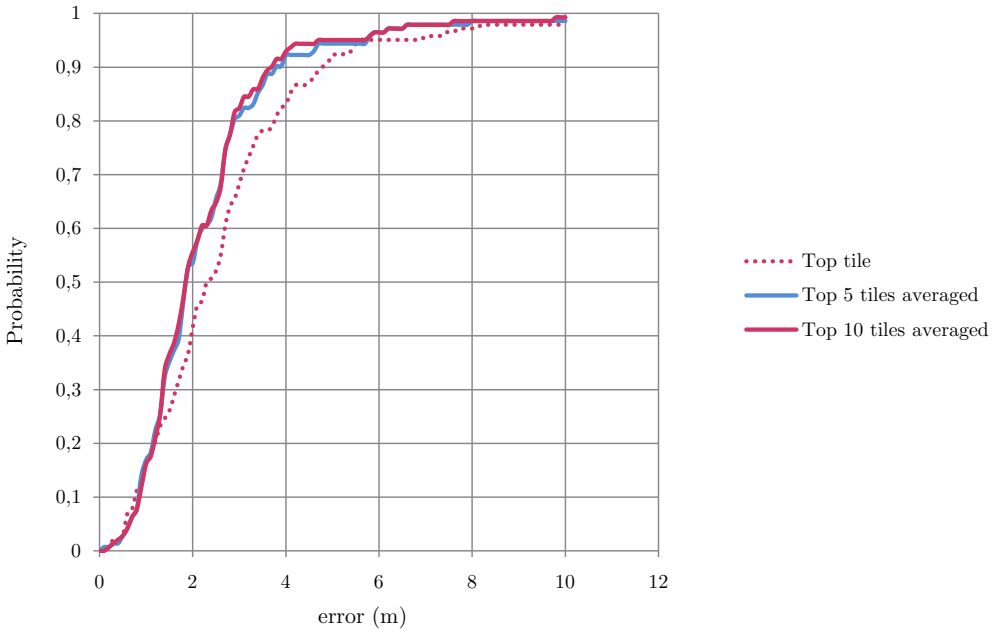

Figure 26: CDF for different amounts of tiles averaged.

An investigation has been made which k would be suitable. A bunch of benchmark tracks are combined in order to investigate a value for k. For $k = 1, 5, 10$ the benchmark routine has been executed. The result can be seen in Figure 26. As one can see, the single top tile

gives inaccurate location results, compared to the weighted averaged top five tiles and top ten tiles. The drawback of the taking the top ten tiles is that locations along the edges of the localization area can be averaged out (not visible in Figure 26). We have chosen to average over the top five tiles, because the localization accuracy is similar to the average of the top ten tiles, which is better then the localization accuracy of the top tile.

5.1.2 Initial benchmarking

The initial benchmarking is used to verify if improvements have positive effect. All benchmark tracks from Figure 25 are used for this initial benchmark. The versions of the localization algorithms used are those described in Section 4.3. The errors for all localization calculations in all windows in all benchmark tracks are combined in a CDF, see Figure 27.

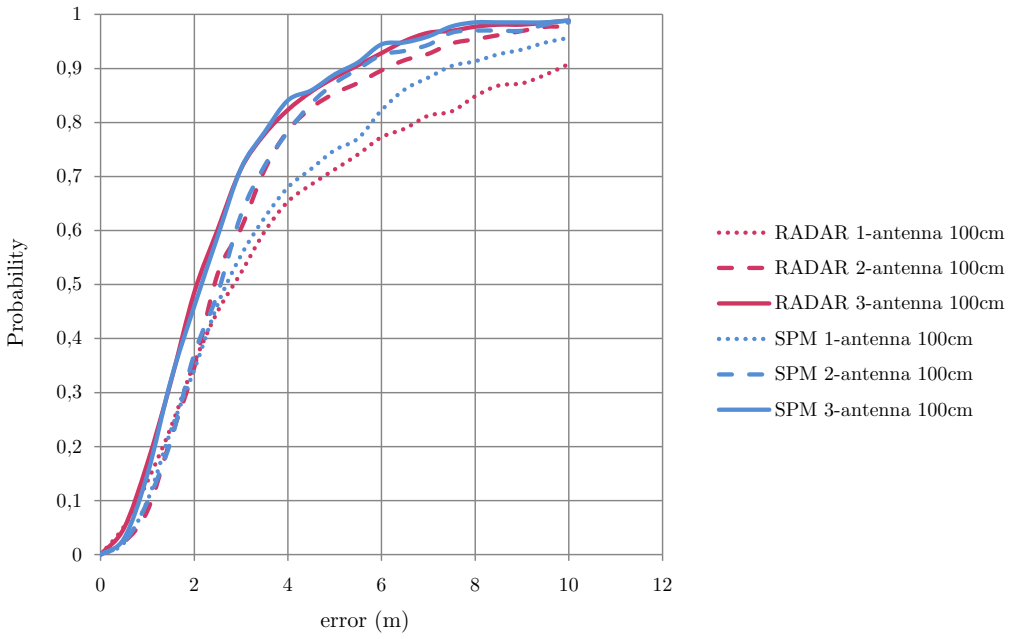

Figure 27: CDF of RADAR and SPM, using $r = 100cm$.

In the *1-antenna* configuration, SPM performs better than RADAR. Namely, the median error (probability = 0.5) for SPM is $< 2.7m$, whereas the median error for RADAR is $< 2.8m$. Also the 80th percentile, SPMs accuracy is $< 5.8m$ against RADAR accuracy of $< 6.8m$. In the *2-antenna* configuration, the 50th percentile error is $< 4.2m$. From then on, SPM prevails. In the *3-antenna* configuration, the difference between RADAR and SPM is even smaller. It can be stated that RADAR and SPM perform similar in the *3-antenna* configuration. The 50th percentile error is $< 2.2m$, and the 80th percentile

error is $< 3.6m$. It was indeed expected that combining radios should indeed perform better than the *1-antenna* configuration. Considering the localization accuracy only, SPM is preferred over RADAR.

The finding that SPM performs better than RADAR confirms the findings of *Kleisouris et al.* However, we did not achieve a localization accuracy as good as theirs. An explanation for this finding is that our setup differs to the setup of *Kleisouris et al.* For SPM, they used a fingerprint database with smaller tiles of $10in$ x $5in$ ($25.4cm$ x $12.7cm$). Another difference in setup is the amount of RSS measurements. Their server waits for at least 350 RSS values for each antenna in order to construct a fingerprint. In our setup, it can be that there is just one or none RSS measurement in the live fingerprint. A third difference in the setups is that we recorded the begin and end location of training and benchmark tracks by clicking on a map on a PC. The inaccuracy of clicking of this map is not compensated. In their setup, they used nine fixed accurate placements at each position to benchmark the system. Besides, we averaged the top five locations whereas *Kleisouris et al.* used the top weighted location. Moreover, for RADAR they used a set of training fingerprints at precisely known locations, whereas we used interpolated fingerprints along the whole localization site. This means that our database contains fingerprints for each individual location, whereas their's did not. This can be the explanation why their results for SPM in *1-antenna* are better (80th percentile error of $2.1m$) than our results ($5.8m$).

5.1.3 Office area versus larger rooms

The CDF shown in the previous section (Figure 27) was based on all benchmark tracks. This section distinguishes the light green tracks (denoted by *office area*) and the dark green tracks (denoted by *larger rooms*). We expect the localization accuracy in larger rooms to be less accurate, because training in larger areas is relative less intensive than in the office area. The localization accuracy in office area and larger rooms is investigated for all *1-antenna*, *2-antenna*, and *3-antenna* multiradio configurations.

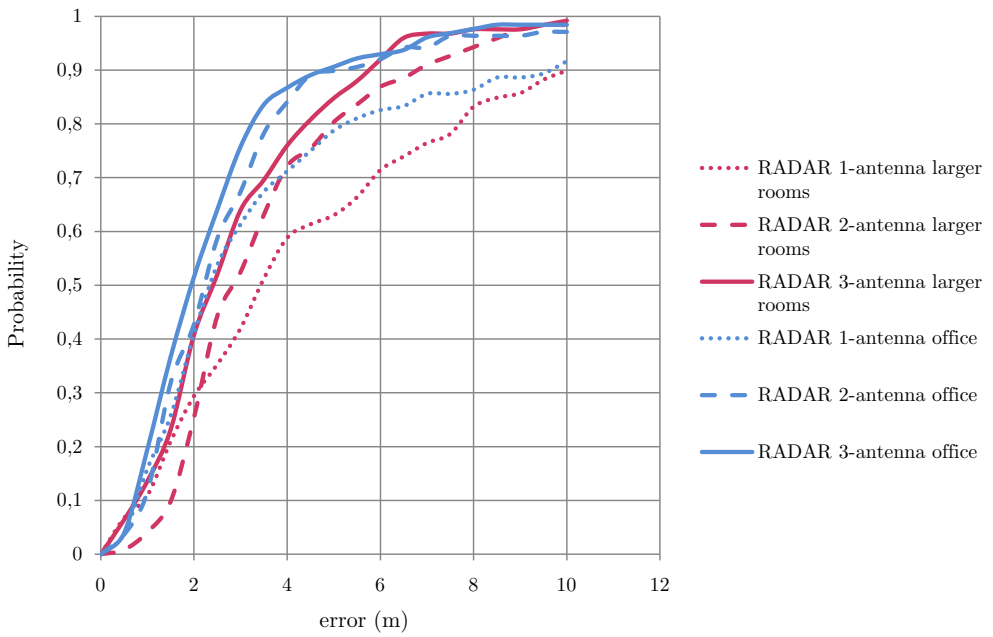

Figure 28: CDFs of RADAR, office area versus larger rooms, $r = 100cm$.

As we can see in Figure 28, all *1-antenna*, *2-antenna*, and *3-antenna* perform better in the office area than in the larger rooms. The 80th percentile error for *1-antenna* is almost $< 7.5m$ in the larger rooms, whereas it is only $< 5.5m$ in the office area (36 % more accurate). For the *2-antenna* configuration we also can see that in the office environment more accuracy can be achieved than in the larger rooms, $< 5.0m$ compared to $< 3.5m$ for the 80th percentile error (43 % more accurate). Finally, the *3-antenna* configuration has similar behavior. The 80th percentile error of the larger rooms is $< 4.5m$, while it is only $< 3.0m$ for the office environment (50 % more accurate). Thus, the 80th percentile error for the office areas is on average 43 % more accurate than in larger rooms.

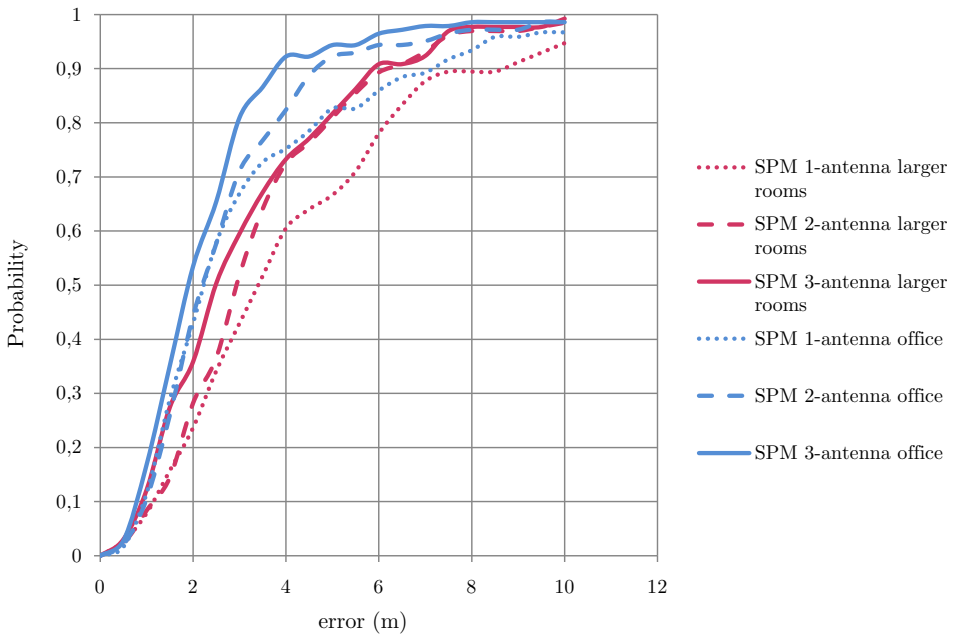

Figure 29: CDFs of SPM, office area versus larger rooms.

For SPM (Figure 29), similar conclusions can be made. The 80th percentile error of *1-antenna* is $< 5.0m$ in the office area, while it is $< 6.5m$ in the larger rooms (30 % more accurate). For *2-antenna* it also holds that office area has a better accuracy ($< 4.0m$) than in the larger rooms ($< 5.0m$, 25% more accurate). The *3-antenna* performs with a 80th percentile error of $< 3.0m$ in the office area, compared to $< 5.0m$ in the larger rooms (67 % more accurate). Thus, the 80th percentile error for the office areas is on average 41 % more accurate than in larger rooms.

Both SPM and RADAR have better localization accuracy in all three antenna configurations. For RADAR and SPM respectively, the 80th percentile localization error in the office environment is on average 43 % and 41 % better than in the larger rooms (averaged of the three radio combinations). This means that whenever a localization site is trained more intensively, a better localization accuracy can be achieved.

5.1.4 Signal map resolution

In the initial benchmarking, we shown that the localization algorithm SPM performs similar to or better than RADAR in all *1-antenna*, *2-antenna*, and *3-antenna* configurations. Nevertheless, it has been shown by *Kleisouris et al.* that SPM can perform better. One of the differences between the setups of *Kleisouris et al.* and the setup used for this thesis, is the size of tiles. The resolution of the fingerprint database is obviously influencing the

localization accuracy. Using our benchmark routine, we benchmarked different fingerprint databases with resolutions of $40cm, 100cm, 200cm, 300cm, 400cm, 500cm$ and $1000cm$, in the *1-antenna* configuration. The same benchmark is done as in the previous cases, only the database's resolution differs, see Figure 30 and Figure 31.

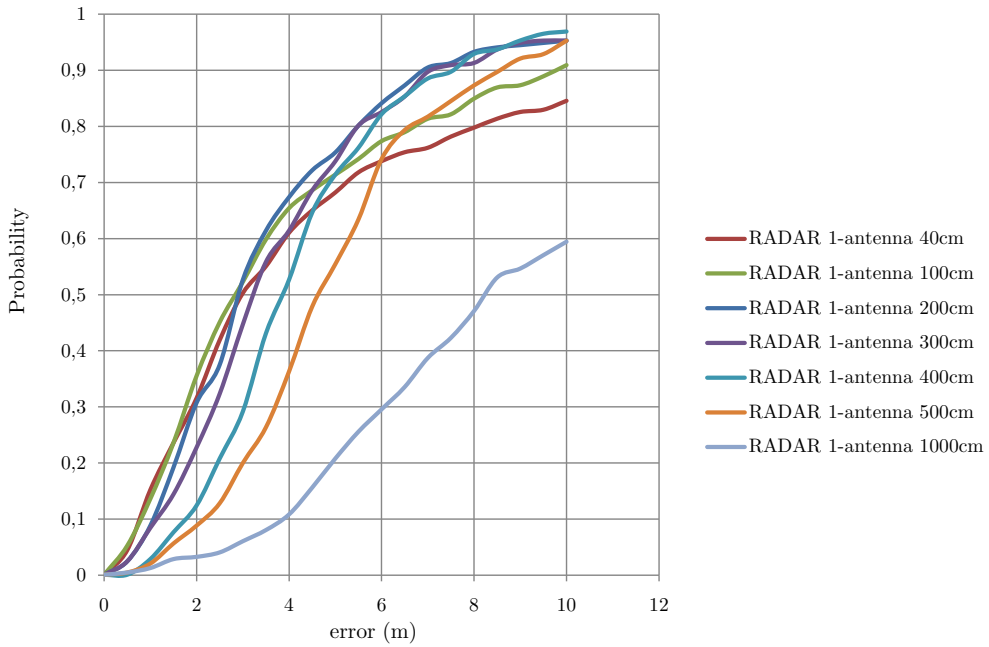

Figure 30: CDFs of RADAR in different resolutions, using *1-antenna* configuration.

Considering Figure 30, we can see that up to the 50th percentile, the databases with resolution of $40cm$, $100cm$ and $200cm$ have the smallest localization errors. From 50th percentile to 95th percentile, the database with resolution of $200cm$ performs best.

For RADAR using *1-antenna*, a database with resolution of $200cm$ is preferred. For SPM, see Figure 31, the databases with resolution of $40cm$, $100cm$, and $200cm$ perform the best.

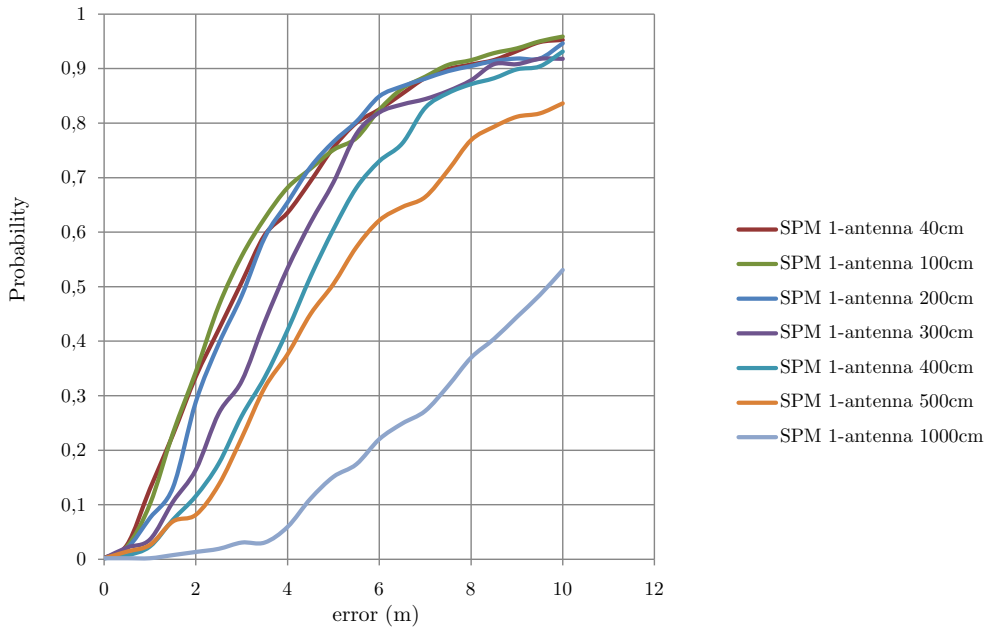

Figure 31: CDFs of SPM in different resolutions, using *1-antenna* configuration.

It can be stated that the database resolution has influence on the localization error. However, both RADAR and SPM perform good with the database with a resolution of $200cm$.

Since we are averaging the top five tiles, we can explain by means of Figure 32 that a too large tile size results in an inaccurate location estimate. In this fictive case the blind node's location is assumed to be at the black dot. Furthermore, we consider a little tile size represented by the red tiles and a large tile size represented by the blue tiles. Note that the outcome of the matching algorithm is assumed to be similar for both the red and blue configuration (since both red and blue tiles surround the blind node similarly). For each color, every weighing of the centroids of the five tiles results in a location estimate which is inside the enclosed square of the tiles of that color. Since the blue tiles are larger, most possible outcomes (of the weighing of the centroids of the blue tiles) are clearly further away from the real location of the blind node than in the red case. Moreover, the maximal possible localization error made by either red or blue is represented by green dots. It is clearly visible that the maximal error of weighing of the blue tiles is bigger. This explains why a tile size of $1000cm \times 1000cm$ performs worse than a tile size of $300cm \times 300cm$.

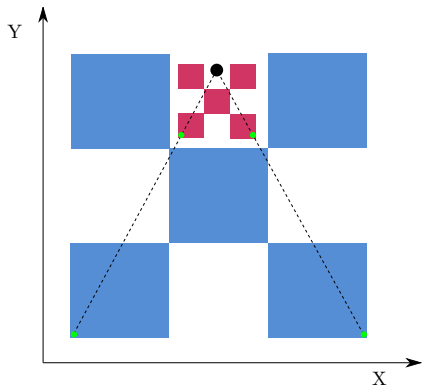

Figure 32: Too big tiles are more inaccurate.

It can also be explained why too small tile sizes give inaccurate localization estimates. Namely, a fingerprint database with a resolution of $200cm$, has let's say k fingerprints in the fingerprint database. If we concern the same localization area, then a fingerprint database with a resolution of $40cm$ has thus $k \cdot (200/40)^2 = k \cdot 25$ fingerprints in the database. Whenever a database is larger, the chance is bigger that the 5 tiles selected are worse since there are more options in the database. Therefore too small tile sizes ($40cm$) cause bad localization accuracy. We think the optimum tile size also depends on the density of RSS training points. Calculating signal maps is based on training points distributed over the localization area. If the density of training points is higher, then the r of the fingerprint database can be smaller.

5.1.5 Adapting RADAR and SPM

The benchmark of RADAR and SPM has shown that the achieved localization accuracy is not as good as *Kleisouris et al.* localization. Differences are described in the Section 5.1.1. In order to reduce the localization error, the following reasoning gives an optimization.

It is known from Chapter 3, that higher RSS values are more accurate than lower RSS values. This can be taken into account by modifying the algorithm. For RADAR, this is done by multiplying the error of each RSS value $E_{x,y}$ with a factor. The factor is a function of the RSS value measured. The function is proportional to the theoretical RSS to distance correlation, see Figure 33a.

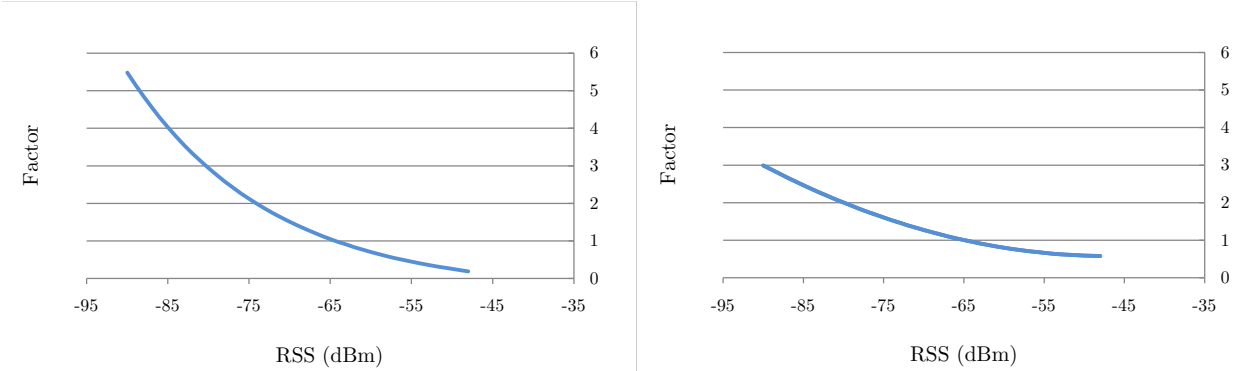

(a) RADAR (b) SPM

Figure 33: Functions improving RADAR and SPM.

A similar factor for SPM is determined as illustrated by Figure 33b. Using experimental guesses for curve fitting in Microsoft Excel, the function is obtained. Again, lower RSS values get a larger δ. Note that the function is slightly flatter than the function for RADAR. This is because the factor for SPM is multiplied by the iteration number. If the factor could reach zero, then the δ can become zero which would mean that almost no tiles are selected.

Using the factors for RADAR and SPM in the way described, is applied and benchmarked in the same way as in previous benchmarks. The benchmark is done for the *1-antenna* and *3-antenna* configurations. The resulting CDFs are shown by Figure 34.

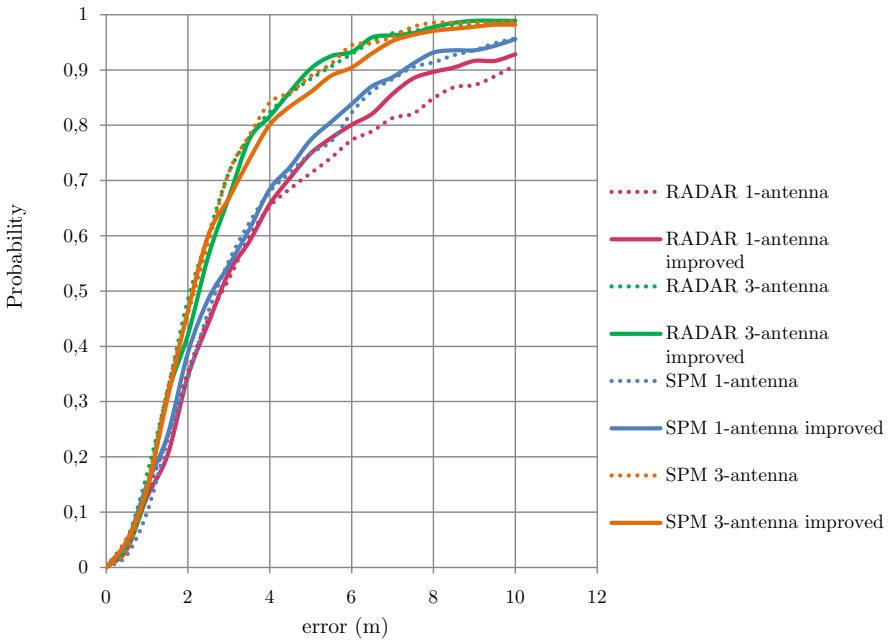

Figure 34: CDFs for improved RADAR and SPM, using $r = 100cm$.

As we can see, the improvements indeed decrease the localization error for the *1-antenna* configuration. For RADAR, the 80th percentile error reduced from $< 7m$ to $< 6m$. SPM's localization accuracy is also improved. The 80th percentile error reduced from $< 6m$ to $< 5.5m$. For the *3-antenna* configuration, it cannot be stated that RADAR's or SPM's localization accuracy improved. RADAR's CDF did not improve or deteriorate. Moreover, the improvement for SPM seems to have negative influence. A possible explanation for the fact that the improvement does not work out for *3-antenna* is that RSS measurements are averaged among the antennas. Therefore the fingerprint which is compared to the database in the *3-antenna* configuration is more accurate than the fingerprint of the *1-antenna* configuration, which could imply that relaxing requirements for matching (e.g. the improvement) does not help anymore.

5.2 Maintenance

Since applicability is a key indicator for practical use, it is investigated how a rebuilding affects signal maps of reference nodes. Obviously, if RSS measurements do not reproduce anymore, the localization system will reasonably fail to operate. Changes in the localization area can cause that RSS measurements do not reproduce anymore.

A case study is done how a rebuilding changes the signal map of a reference node. Then, it is reasoned how changes in the signal map can be detected. If detected, the installation

engineer will have to cope with a retraining of the localization site.

On forehand, one can imagine that the a rebuilding changes the signal power distribution of reference nodes. During the thesis phase, there was a rebuilding at AME.

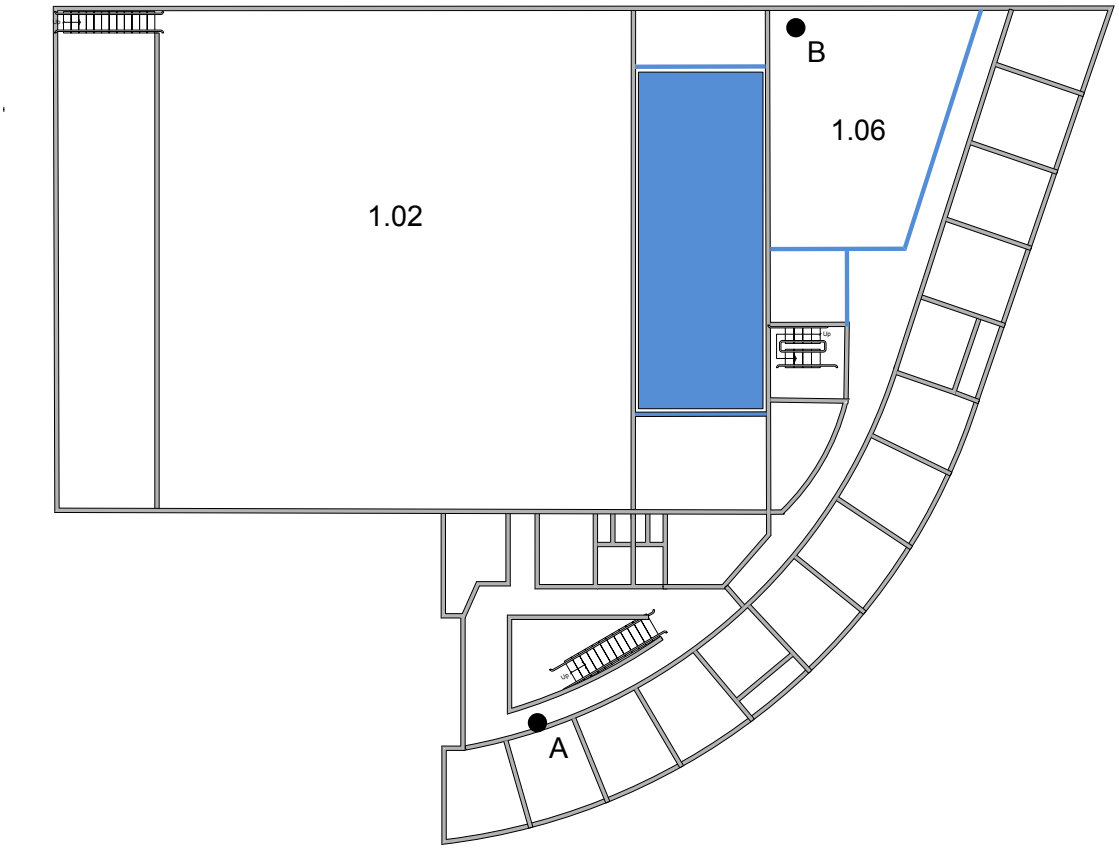

Figure 35: Blue shaded walls and roofs have changed during the rebuilding.

For this section, only room 1.06, the offices along the right and the corridors are considered.

Figure 35 shows the parts of the building that were rebuilt. Room 1.06, the canteen, was changed to a lab environment with Electrostatic Discharge (ESD) floor. For safety reasons, this required construction of new walls, indicated by surrounding blue lines. A new canteen is placed where the terrace at the first floor was located. This means that this roof terrace was roofed and walls were placed. The new canteen is depicted by the blue square in the figure.

For two reference nodes A and B, it is investigated how the signal maps have changed due to the rebuilding. Obviously, the orientation and position of A and B is equal before and after rebuilding. Before and after the rebuilding took place, signal maps are built for A

and B. The signal map from before rebuilding is subtracted from the signal map after rebuilding. The signal maps built before rebuilding were built using RSS measurements from a Stick, and the signal maps built after rebuilding were built using RSS measurements from the target hardware, called the AME Sensor Node.

Node A was placed at $(28.6m, 42.6m)$ at a height of $2.7m$ and a node B was placed at $(43.3m, 1.6m)$ at a height of $2.7m$, as depicted by Figure 35. Node A is located tens of meters from the rebuilding, whereas node B is located exactly in the part of the building which was rebuilt. The expectation is that the signal map of node A was not too much influenced by the rebuilding, and that the signal map of node B was emphatically influenced by the rebuilding.

The result of subtracting the signal map from before the rebuilding from the signal map from after rebuilding, is drawn in Figure 37 and Figure 38. For both figures, the color mapping depicted by Figure 36 applies. Thus, a green or yellow color represents the case that the RSS value is higher after rebuilding. The orange color represents that there is not too much difference after rebuilding. The red color indicates that the RSS value before rebuilding is higher than after rebuilding.

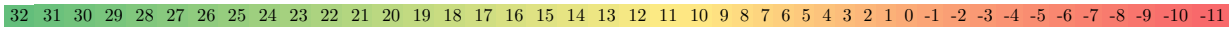

Figure 36: Color mapping for Figure 37 and Figure 38.

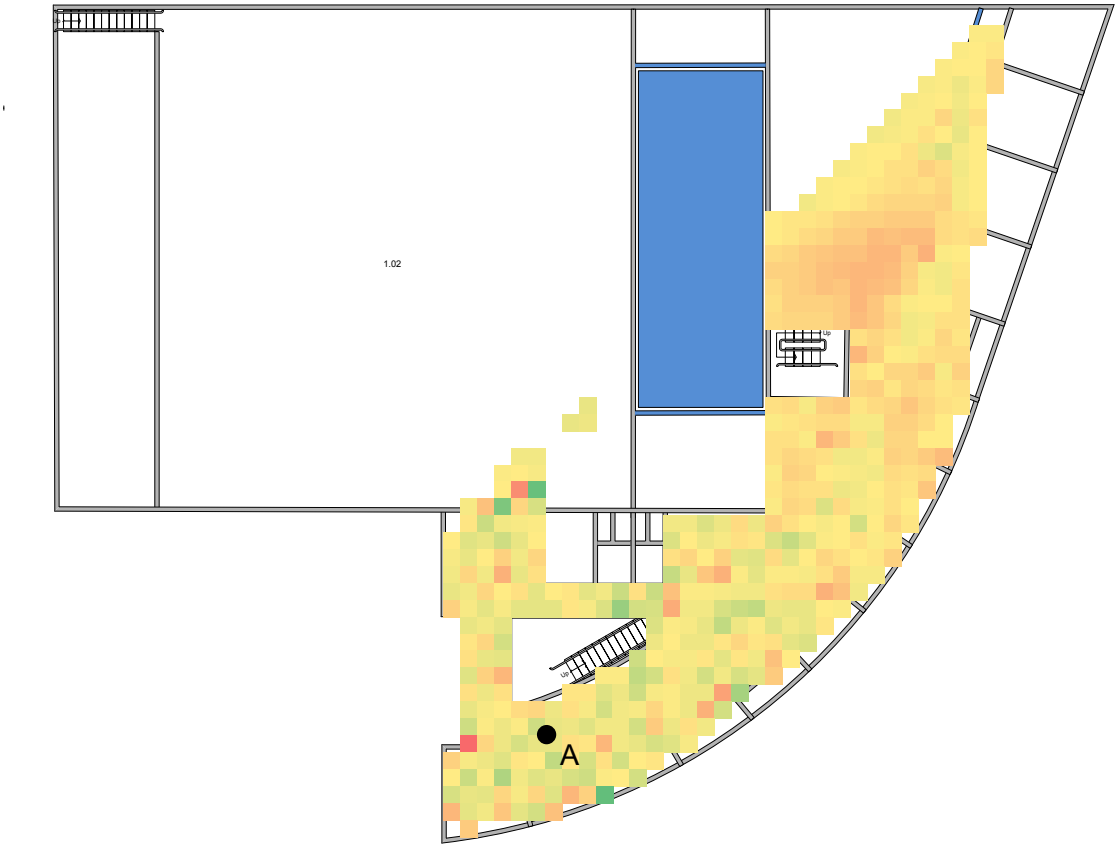

Figure 37: Difference of signal map of node A.

Figure 37 shows the difference of signal maps of reference node A. As one can see, the yellow color dominates, which means that the RSS values expected after rebuilding are higher. This comes due to the fact that the training after the rebuilding was done with an AME Sensor Node which has different hardware than the Stick. Namely, the AME Sensor Node is equipped with a more sensitive ZigBee radio than the Stick. Besides the yellow color, we can see few other differences, indicted by red and green spots. This can be explained by movements in the localization site. Namely, all employees are rearranged over the offices during rebuilding. This rearrangement includes movements of small office cupboards. Since difference of the signal maps does not show high variation, we think this does not indicate big changes in the localization site.

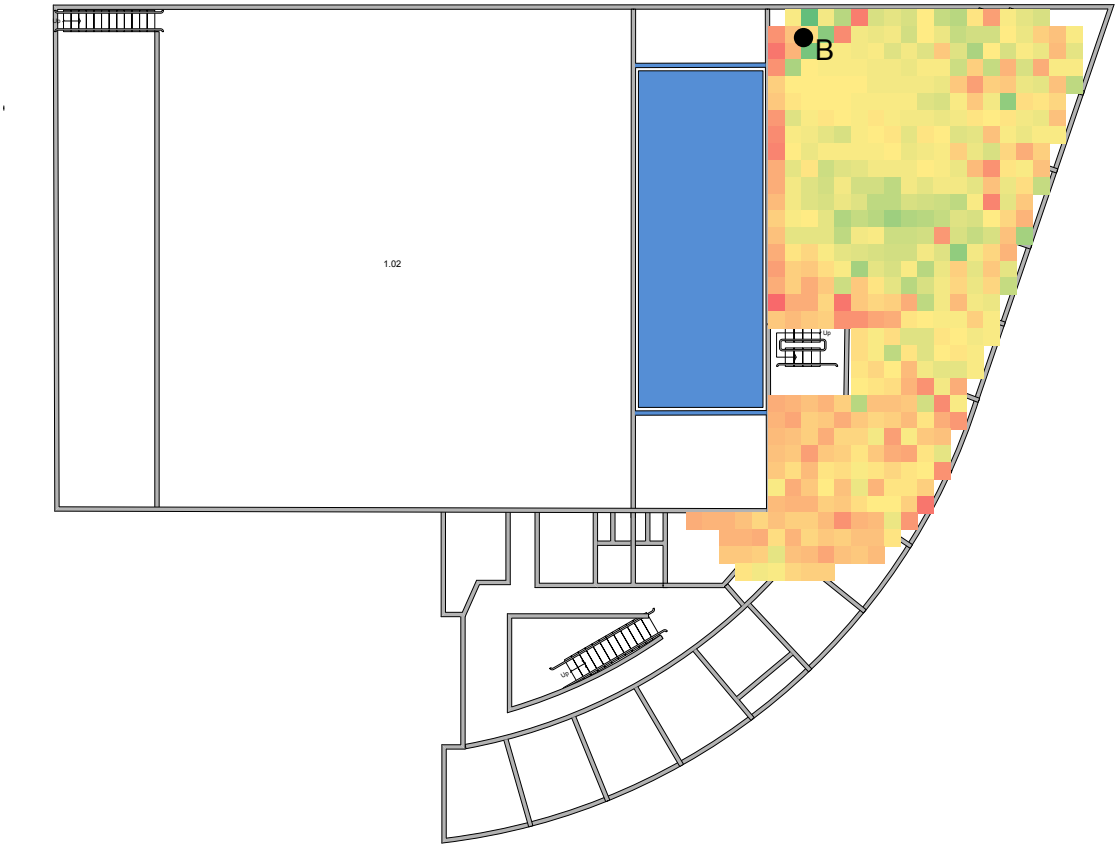

Figure 38: Difference of signal map of node B.

Considering the difference of signal maps of node B (Figure 38), we see more variation in the difference of signal maps from before and after the rebuilding. One can see meshes of orange and yellow, and a number of red and green spots. This certainly indicates that there have been big changes. Indeed, the rebuilding affects the part of signal map where rebuilding took place, but also the offices and other surrounding area.

Concluding this section, rebuilding strongly influences signal maps of neighboring nodes. This means that whenever a big change in the localization area takes place, the signal maps of these reference nodes should be rebuilt. This can be done by retraining. The question is when to decide that a new training is desired. The answer to this question is left as future work.

5.3 Conclusion

The proposed localization system is evaluated by benchmark routine. Based on practical RSS measurements, the system is benchmarked. The metrics of interest are the resolution of the database (since this is lineair in the size of the database), the multiradio configuration, and the corresponding localization accuracy.

It was shown that the *1-antenna* combination is outperformed by *2-antenna* and *3-antenna*, thus multiradio is preferred. Including basic improvements, the RADAR matching algorithm performs with an 80th percentile error of $< 6m$, for the *1-antenna* configuration. SPM performs better, having an 80th percentile error of $< 5m$. Combining three ZigBee radios (*3-antenna* configuration) gives a better localization accuracy. Namely, using RADAR or SPM gives an 80th percentile error of $< 4m$.

When only localization accuracy is the metric of interest, SPM is preferred. However, SPM is a recursive algorithm which implies that the fingerprint database can be iterated multiple times before any localization result is there. In contrast to SPM, RADAR guarantees that the database is iterated exactly once (which takes $1.25sec$ in our basic experiment, mentioned in Section 4.3.1). If SPM needs let's say three iterations, then the running time of SPM would be $1.25 \times 3 = 3.75sec$, which is not realtime in our opinion. Based on this guarantee and the fact that the implementation of RADAR is slightly easier (since it does not have to maintain sets of tiles), RADAR is chosen for first implementation of the embedded software of the AME Sensor Node.

A trade-off between localization accuracy and running time can be made. For *1-antenna* RADAR is as good as SPM, but since we are committed to running time and having a localization result, we prefer RADAR.

6 Discussion

The goal of this thesis was to present *a scalable indoor location tracking system with room-level accuracy (3m)*. The term *scalable* was in the context of number of blind nodes. Theoretically, infinitively many blind nodes can be used by the proposed localization scheme. A blind node only "listens" to reference nodes, thus no network load is added when a blind node is localizing. The goal of $3m$ localization accuracy is achieved for the 75th percentile error, using the *3-antenna* configuration of either SPM or RADAR (see Figure 34 in Section 5.1.5). However, this goal is not yet met for the AME Sensor Node.

To adopt the system in an existing AME ZigBee network, we only have to update the embedded software of the existing nodes. All AME ZigBee products can be used as reference node, regardless of their signal power distribution. Both adoptability (Requirement 2 (Adoptability of existing AME ZigBee devices)) and embedded localization (Requirement 3 (Scalability in nr. of blind nodes) and Requirement 6 (Calculations by blind node)) are completely fulfilled.

The blind node's environmental knowledge is minimal, i.e. it only knows expected signal strengths along the localization site (Requirement 4 (Blind node has no environmental knowledge)). Even the location of reference nodes is not known by the blind node.

The blind node's hardware is based on the AME Sensor Node. It is perfect for person or object tracking since its dimensions are limited (fulfilling Requirement 1 (Suitable for realtime person tracking)). It has been shown that a rebuilding affects signal maps of reference nodes. The signal maps of reference nodes near the rebuilding are highly affected. The signal maps of reference nodes tens of meters distanced from the rebuilding.

The localization scheme has been completed and benchmarked. The postprocessing can be extended in the future. One can easily let the system react on situations for specific locations (Requirement 5 (Enhancements for specific location)).

6.1 Contributions

The localization system presented in this thesis differs from other WSN localization techniques in a couple of ways.

At first, the scalability of the system is a point to highlight. Where other WSN based localization system use a central server [2], in the presented solution blind nodes can localize themselves without sending any message to the network. A blind node only needs to "listen" to the network in order to calculate its location. This means that any number of blind nodes can be used to localize itself. This is just like the GPS system, where infinitively many blind nodes (car navigation, aircrafts, tracking devices etcetera) can localize themselves without sending messages back to the GPS satellites.

Adoptability is also a key property of the proposed system. In order to use an existing AME ZigBee device as a reference node, the device only needs to periodically send "beacon messages". A beacon message is a 1-hop beacon message sent at the MAC layer of the OSI model, which is beneath the network layer. This implies that a blind node can listen to beacon messages from reference nodes of other networks. Besides having a static location, sending messages is the only assumption made for existing AME ZigBee devices to operate as reference node. Note that the size, application and even network of reference devices can be arbitrary. Only a software update is needed in order to let an arbitrary AME ZigBee device function as a reference node.

The localization accuracy is improvable without changing reference nodes. Usual localization techniques require adjustments of hardware or software of reference nodes. The localization system proposed by this thesis can be improved by only adding one or more ZigBee radios to the blind node. The hardware design of the blind node enables support for mounting an additional printed circuit board (PCB), where an additional ZigBee radio can be connected to. In case of adding two ZigBee radios to a blind node, the median localization accuracy can increase from $3m$ to $2m$. This is when using an adapted version of the SPM algorithm. Also, over-the-air updates of embedded software of a blind node are possible, which gives possibility to improve the accuracy later on.

In short, the proposed system offers a scalable solution to indoor localization which can be adopted in existing AME ZigBee networks.

6.2 Future work

It has been shown that a rebuilding affects the signal maps of reference nodes. However, the influence of changes in the localization site are not fully explored. Namely, the Achilles heel of the system is that major changes of the localization area can cause the system to fail. An interesting topic is the maintenance of the fingerprint database. Industrial environments can change frequently, which implies that a retraining must be done. The question is to what extend a rebuilding or change in localization site will affect the localization accuracy, and moreover how this can be detected. An idea is that (some) reference nodes are getting functionality to detect major changes in the signal maps. For example, if a reference node also measures RSS values from neighboring nodes, it can verify whether RSS values vary over time. If (a group of) reference nodes has detected that there is significant change in RSS values, a retraining should be done.

Improving localization accuracy can also be investigated. As *Kleisouris et al.* show, accuracy can be improved by assuming a gaussian distribution of RSS measurements over the localization site. Besides, speeding up the sendrate of reference nodes sending beacons will reasonably lead to better accuracy. A blind node then will receive more RSS values, averaging out errors. The blind node which is currently targeted to be an AME Sensor

Node, is equipped with an accelerometer. This accelerometer can be used for postprocessing. The mathematical derivation of acceleration is speed and can be derived to distance. Then, the location calculation can be enhanced by taking distance into account.

References

[1] K. Aamodt. CC2431 Location Engine, Application Note AN042 Texas Instruments. July 2006.

[2] P. Bahl and V.N. Padmanabhan. RADAR: an in-building RF-based user location and tracking system. In *INFOCOM 2000. Nineteenth Annual Joint Conference of the IEEE Computer and Communications Societies. Proceedings. IEEE*, volume 2, pages 775 –784 vol.2, 2000. doi: 10.1109/INFCOM.2000.832252.

[3] S. Biaz, Ji. Yiming, Bing Qi, and Shaoen Wu. Dynamic signal strength estimates for indoor wireless communications. In *Wireless Communications, Networking and Mobile Computing, 2005. Proceedings. 2005 International Conference on*, volume 1, pages 602 – 605, September 2005. doi: 10.1109/WCNM.2005.1544117.

[4] Youssef Chraibi. Localization in wireless sensor networks. 2005. Master's Thesis, Stockholm University Sweden.

[5] H.B.M. Derks. Specification graduation project. Internal document Applied Micro Electronics "AME" BV and Eindhoven University of Technology, May 2011. Available on request.

[6] E. Elnahrawy, Xiaoyan Li, and R.P. Martin. The limits of localization using signal strength: a comparative study. In *Sensor and Ad Hoc Communications and Networks, 2004. IEEE SECON 2004. 2004 First Annual IEEE Communications Society Conference on*, pages 406 – 414, Oct. 2004. doi: 10.1109/SAHCN.2004.1381942.

[7] F. Kirsch and M. Vossiek. Distributed kalman filter for precise and robust clock synchronization in wireless networks. In *Radio and Wireless Symposium, 2009. RWS '09. IEEE*, pages 482 –485, Jan. 2009. doi: 10.1109/RWS.2009.4957393.

[8] K. Kleisouris, Yingying Chen, Jie Yang, and R.P. Martin. Empirical Evaluation of Wireless Localization when Using Multiple Antennas. *IEEE Transactions on Parallel and Distributed Systems*, 21(11):1595 –1610, November 2010. ISSN 1045-9219. doi: 10.1109/TPDS.2010.39.

[9] Erin-Ee-Lin Lau and Wan-Young Chung. Enhanced RSSI-Based Real-Time User Location Tracking System for Indoor and Outdoor Environments. In *Convergence Information Technology, 2007. International Conference on*, pages 1213 –1218, November 2007. doi: 10.1109/ICCIT.2007.253.

[10] Asis Nasipuri and Kai Li. A directionality based location discovery scheme for wireless sensor networks. In *Proceedings of the 1st ACM international workshop on Wireless sensor networks and applications*, WSNA '02, pages 105–111, New York, NY, USA,

2002. ACM. ISBN 1-58113-589-0. URL http://doi.acm.org/10.1145/570738.570754.

[11] Vinod Patmanathan. Area Localization using WLAN. 2006. Master's Thesis, Stockholm University Sweden.

[12] Qubulus. Qubulus, indoor positioning service provider. http://www.qubulus.com, 2011. Accessed July 1, 2011.

[13] S. Schwarzer, M. Vossiek, M. Pichler, and A. Stelzer. Precise distance measurement with IEEE 802.15.4 (zigbee) devices. In *Radio and Wireless Symposium, 2008 IEEE*, pages 779 –782, January 2008. doi: 10.1109/RWS.2008.4463608.

[14] Navin Kumar Sharma. A weighted center of mass based trilateration approach for locating wireless devices in indoor environment. In *Proceedings of the 4th ACM international workshop on Mobility management and wireless access*, MobiWac '06, pages 112–115, New York, NY, USA, 2006. ACM. ISBN 1-59593-488-X. URL http://doi.acm.org/10.1145/1164783.1164804.

[15] Adam Smith, Hari Balakrishnan, Michel Goraczko, and Nissanka Priyantha. Tracking moving devices with the cricket location system. In *Proceedings of the 2nd international conference on Mobile systems, applications, and services*, MobiSys '04, pages 190–202, New York, NY, USA, 2004. ACM. ISBN 1-58113-793-1. doi: http://doi.acm.org/10.1145/990064.990088.

[16] Nanotron Technologies. Real Time Location Systems (RTLS). White paper, http://www.nanotron.com/EN/pdf/WP_RTLS.pdf, May 2007.

[17] Maarten Weyn. *Opportunistic Seamless Localization.* PhD thesis, University of Antwerp, 2011.

[18] J. Wittwer, F. Kirsch, and M. Vossiek. A distance-bounding concept for bilateral ieee 802.15.4 communication. In *Microwaves, Communications, Antennas and Electronics Systems, 2009. COMCAS 2009. IEEE International Conference on*, pages 1 –4, nov. 2009. doi: 10.1109/COMCAS.2009.5385999.

[19] J. Wittwer, F. Kirsch, and M. Vossiek. A distance-bounding concept for bilateral IEEE 802.15.4 communication. In *Microwaves, Communications, Antennas and Electronics Systems, 2009. COMCAS 2009. IEEE International Conference on*, pages 1 –4, November 2009. doi: 10.1109/COMCAS.2009.5385999.